Provenance analysis of the Voirons Flysch (Gurnigel nappe, Haute-Savoie, France): stratigraphic and palaeogeographic implications

Jérémy Ragusa, Pascal Kindler, Branimir Segvic & Lina Maria Ospina-Ostios

International Journal of Earth Sciences
GR Geologische Rundschau

ISSN 1437-3254

Int J Earth Sci (Geol Rundsch)
DOI 10.1007/s00531-017-1474-9

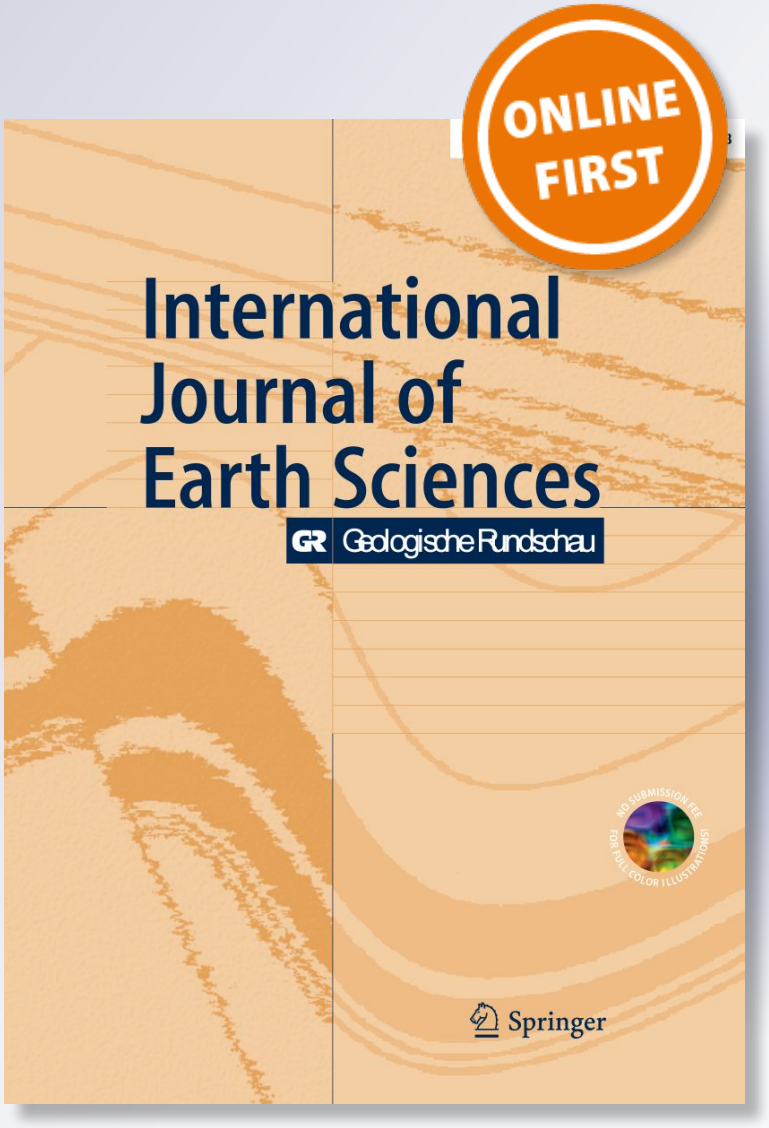

Springer

Int J Earth Sci (Geol Rundsch)
DOI 10.1007/s00531-017-1474-9

REVIEW ARTICLE

Provenance analysis of the Voirons Flysch (Gurnigel nappe, Haute-Savoie, France): stratigraphic and palaeogeographic implications

Jérémy Ragusa[1] · Pascal Kindler[1] · Branimir Segvic[2] · Lina Maria Ospina-Ostios[3]

Received: 19 December 2016 / Accepted: 26 March 2017

Abstract The Chablais Prealps (Haute-Savoie, France) represent a well-preserved accretionary wedge of the Western Alpine Tethys. They comprise a stack of sedimentary nappes related to palaeogeographic realms ranging from the Ultrahelvetic to the Southern Penninic. The provenance analysis is based on the Gazzi-Dickinson method and on QEMSCAN® for heavy-minerals. The Quartzose petrofacies is the most important of the two sources, and supplied three of the four formations of the Voirons Flysch. It is similar to the sources that fed the other flyschs from the Gurnigel nappe. It is characterised by a mature, quartz-rich assemblage and a heavy-mineral population dominated by apatite and the zircon–tourmaline–rutile mineral group. These observations suggest a Clastic wedge provenance. The Feldspathic petrofacies is derived from a feldspar-rich source associated with metamorphic clasts and a heavy-mineral population dominated by garnet. This provenance characterises only one formation of the Voirons Flysch, and is related to the axial belt provenance. This provenance analysis shows that the Middle Eocene to Early Oligocene Voirons Flysch was fed by two sources, in contrast to the other flyschs of the Gurnigel nappe, and further suggests that this flysch was not deposited in the Piemont Ocean but in the Valais domain. Based on the results and comparative provenance analysis with the other flyschs of the Gurnigel nappe, we propose a generic feeding model which involves the Sesia–Dent Blanche nappe, the sedimentary nappes incorporated in the accretionary prism, and probably the Briançonnais basement.

Keywords Gurnigel nappe · Chablais Prealps · Voirons Flysch · Provenance · QEMSCAN · Heavy-mineral · Valais domain

Introduction

The Alps are one of the most studied mountain chains in the world, and recent palaeogeographic reconstitutions have shed light on the distribution of tectonic units and the timing of their incorporation into the orogenic belt (Schmid et al. 1996, 2004; Stampfli and Borel 2002; Stampfli et al. 2002; Handy et al. 2010). The palaeogeographic reconstructions of sedimentary covers are partly based on age data, with the youngest age indicating the end of sedimentation in the basin and its subsequent incorporation into the accretionary prism (Stampfli et al. 2002). Most of these youngest and highest sedimentary successions essentially consist of flysch deposits. Provenance studies on the extrabasinal detrital fraction of these flyschs are highly used for palaeogeographic reconstructions. These studies normally rely on petrographic and mineralogical analogies with hypothesised source materials (von Eynatten and Gaupp 1999; Beltran-Trivino et al. 2013) which help to establish the sedimentary flux and to estimate the successive exhumation of the detrital sources through time (Trautwein et al. 2001). The techniques of

Electronic supplementary material The online version of this article (doi:10.1007/s00531-017-1474-9) contains supplementary material, which is available to authorized users.

✉ Jérémy Ragusa
jeremy.ragusa@unige.ch

[1] Department of Earth Sciences, University of Geneva, 13, Rue des Maraîchers, 1205 Geneva, Switzerland

[2] Department of Geosciences, Texas Tech University, 1200 Memorial Circle, Lubbock, TX 79409, USA

[3] Universidad del Valle, Escuela de Ingeniería Civil y Geomática, Cali, Colombia

Published online: 12 April 2017

provenance analysis have markedly improved in the last decades with the refinement of the tectonic settings of the source rocks (Dickinson and Suczek 1979; Dickinson et al. 1983; and; Dickinson 1985), the development of statistical tools to constrain the sediment source (Garzanti et al. 2004, 2007, 2010; Garzanti and Andó 2007) and the geochemistry of single grains (von Eynatten and Dunkl 2012).

In the Alps, many sedimentary cover nappes are separated from their crystalline basement which complicates the identification of their original palaeogeographic location. In particular, the palaeo-depositional realm of the Cretaceous to Eocene Gurnigel nappe, a flysch nappe now exposed in the Swiss and French Prealps (Fig. 1), is most controversial, as it has been successively placed in the Ultrahelvetic domain (Lombard 1940; Hsü 1960; Trümpy 1960; Hubert 1967; Hsü and Schlanger 1971), along the southern margin of the Piemont Ocean (Caron 1976; Winkler 1983, 1984), and, more recently, in the Valais trough (Trümpy 2006; Ospina-Ostios et al. 2013; Ragusa 2015) (Fig. 2).

The goal of this study is to analyse the framework composition and heavy-mineral assemblage of the Middle Eocene to Early Oligocene Voirons Flysch which corresponds to the western extension of the Gurnigel nappe in France (Fig. 1). These new data provide unsuspected information on the source regions of this flysch, and help in refining its stratigraphical context. Data are further compared with similar results from other parts of the Gurnigel nappe and from various Prealps flyschs (Figs. 1, 2; Caron et al. 1989), and finally are used to formulate an original palaeogeographic model for the Voirons Flysch.

Geological background

The Prealps form moderately elevated reliefs (ca. 2000 m) between Lake Geneva and Lake Zurich (Fig. 1). They include, in particular, the Chablais massif, south of Lake Geneva, and the Swiss Prealps, between Lake Geneva and Lake Thun. These reliefs encompass a stack of sedimentary

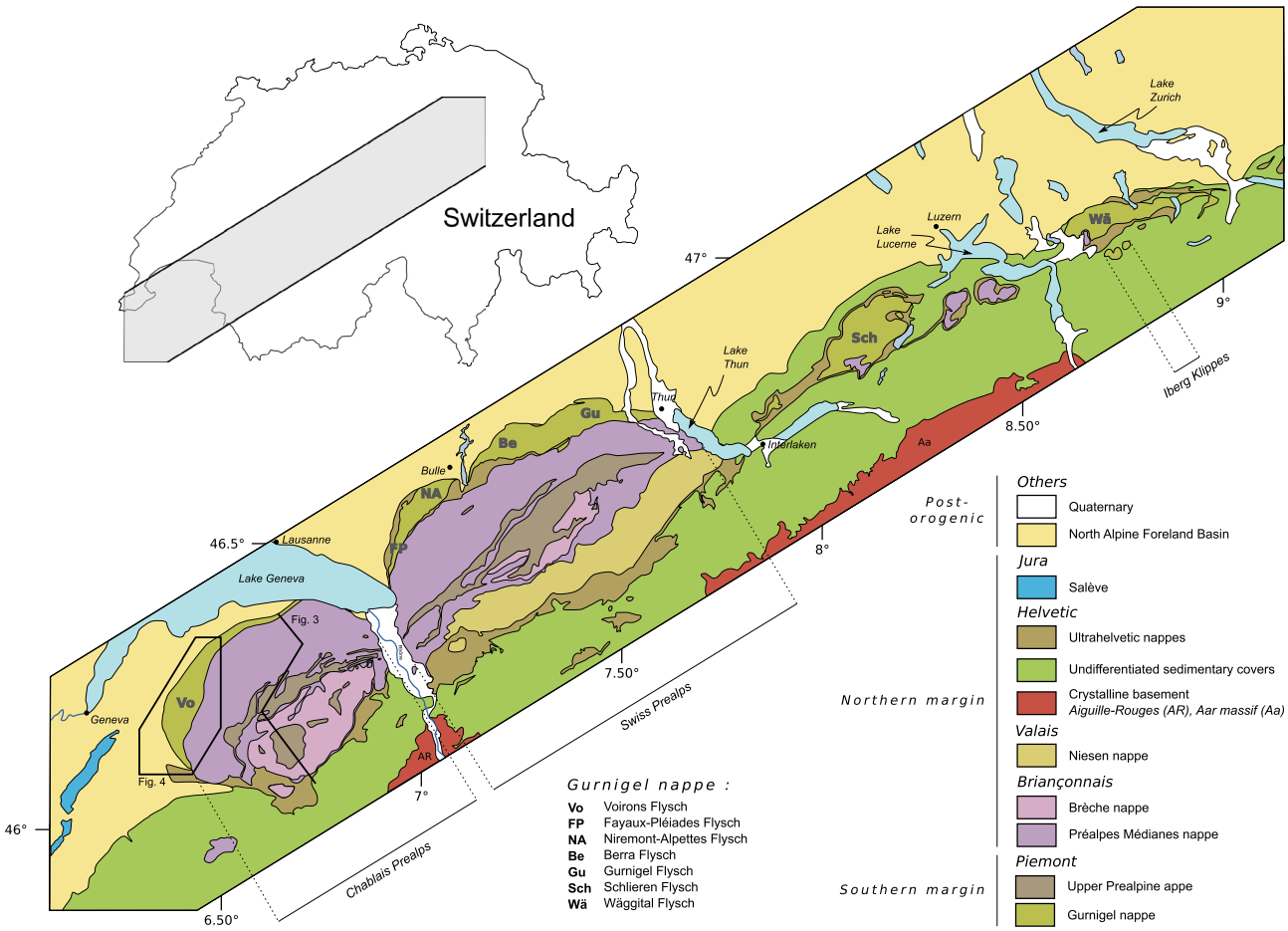

Fig. 1 Tectonic map of the Chablais and Swiss Prealps (SwissTopo 2008, modified) with the location of the different flyschs of the Gurnigel nappe. The *black box* indicates the studied area described in Fig. 4

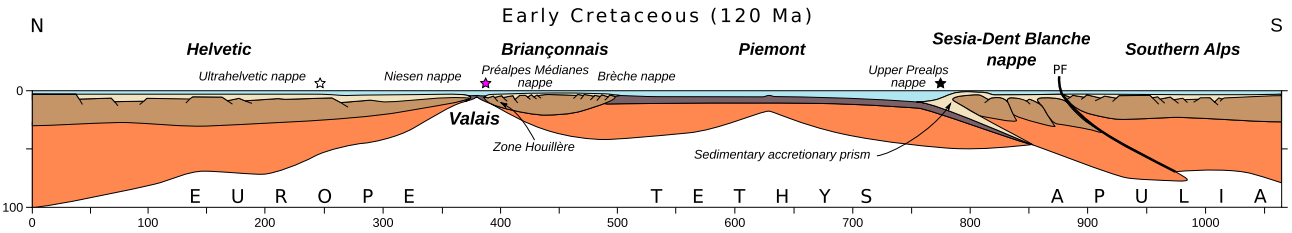

Fig. 2 Simplified palinspastic model from Stampfli et al. (1998, modified) with the original location of the Prealps nappes. Stars represent the successive paleogeographic attribution of the Gurnige nappe: Ultrahelvetic realm (*white*), South Penninic (*black*) and Valais domain (*purple*)

cover nappes detached from their respective basement during the Alpine subduction, and follow a thin-skinned, in-sequence thrusting (Figs. 1, 3; Mosar 1991; Wissing and Pfiffner 2002). They represent the former sedimentary accretionary to orogenic prism of the Alpine Tethys in this part of the Western Alps (Stampfli et al. 1998; Handy et al. 2010). Nowadays, they overlie the Helvetic nappes to the SE and the North Alpine Foreland Basin (NAFB) to the NW (Fig. 1). Due to the NW translation of both of these units, the frontal edge of the Prealps includes tectonic slices from the Helvetic nappes (e.g. the Subalpine Flysch) and from the subsequent filling-up of the NAFB (e.g. the Subalpine Molasse). These units are separated from the Prealps nappes by the Infraprealpine mélange (Fig. 4; Jeanbourquin et al. 1992).

The Gurnigel nappe is one of the lowermost nappes of the Prealps, and is exposed along their NW edge (Figs. 1, 3). It comprises several flysch units generally interpreted as gravity-flow deposits: Voirons (Lombard 1940; Ospina-Ostios et al. 2013; Ragusa 2015), Fayaux (Van Stuijvenberg 1976; Weidmann et al. 1976; Jan du Chêne 1977; Weidmann 1985), Niremont (Morel 1980; Ambrosetti 2005), Berra (Tercier 1928), Gurnigel (Van Stuijvenberg 1979), Schlieren (Winkler 1983, 1984, 1993) and Wägital (Winkler et al. 1985b). These different flysch successions share similar lithostratigraphic characteristics. Indeed, previous mineralogical studies in the Gurnigel (Van Stuijvenberg 1979), Schlieren (Winkler 1983, 1984) and Wägital (Winkler et al. 1985b) flyschs show that constituent rocks are characterised by a quartz-feldspar-dominated modal composition with subordinate lithics and a heavy-mineral population dominated by zircon-tourmaline-rutile (ZTR) and garnet (Wildi 1985). The presence of peculiar agglutinated foraminifers (*Rhabdamina* fauna; Brouwner 1965; Weidmann 1967; Van Stuijvenberg et al. 1976; Ujetz 1996), the nature of bioturbations (Crimes et al. 1981), and the sedimentological features (Kuenen and Carozzi 1953), all suggest a deep-marine sedimentary environment for these successions. Early biostratigraphic studies based on calcareous nannofossils, dinoflagellates and, more rarely, on planktonic foraminifers indicated a Late Maastrichtian to Lutetian age for all flysch units of the Gurnigel nappe (Rigassi 1958; Kuhn 1972; Jan du Chêne et al. 1975; Jan du Chêne 1977; Van Stuijvenberg 1979; Winkler 1983, 1984, 1990; De; Kaenel et al. 1989). Such an age range is also supported by the occurrence of bentonite layers dated from the Paleocene in the lower part of the Schlieren Flysch (Winkler et al. 1985a; Koch et al. 2015), and possibly related to the North Atlantic events (Egger et al. 2005). However, planktonic foraminifers of Middle to Late Eocene/Early Oligocene age have recently been retrieved from the Voirons Flysch (Ujetz 1996; Ospina-Ostios et al. 2013).

For long, the flysch units outcropping along the NW edge of the Prealps were thought to originate from the Ultrahelvetic realm (e.g. Tercier 1928; Lombard 1940; Fig. 2), but several authors had already noticed the petrographical resemblance of some conglomerate clasts found in these units (e.g. pink granite fragments) with several

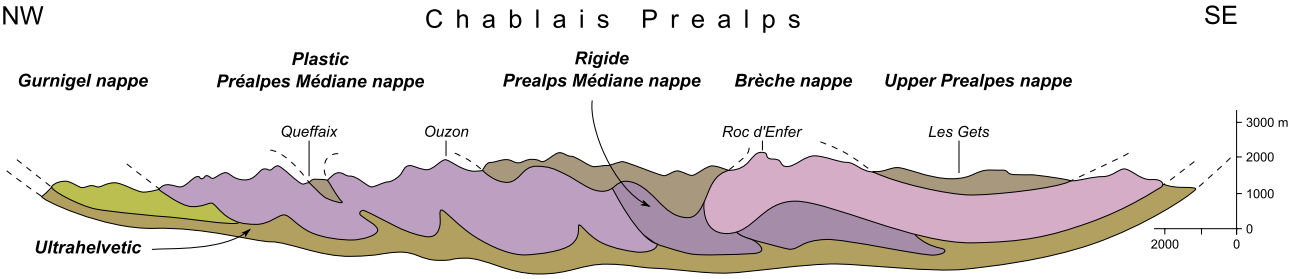

Fig. 3 Cross section of the Chablais Prealps from Caron (1972, modified)

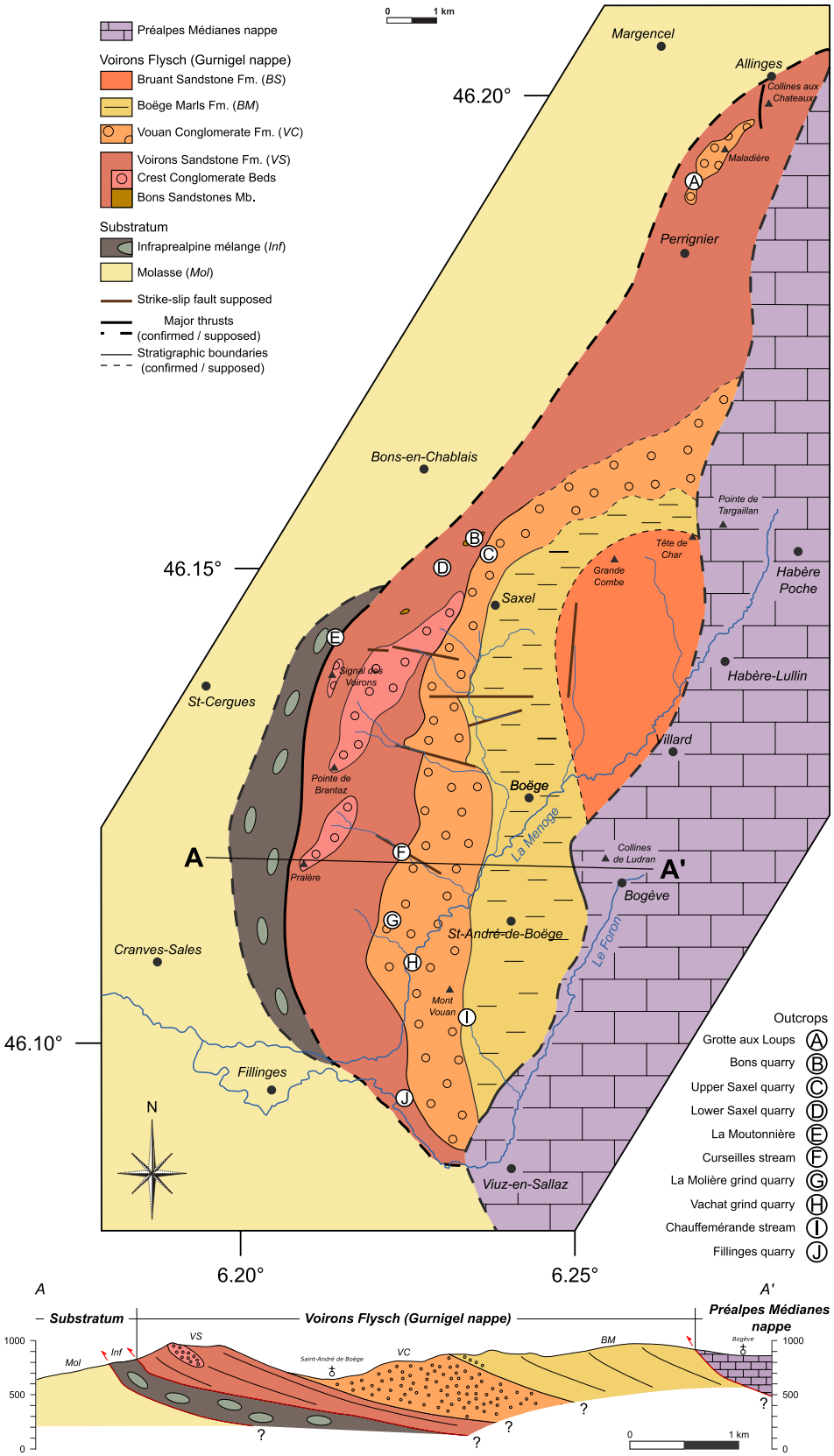

Fig. 4 Tectonic map of the Voirons Flysch and associated cross section. *Outcrops* mentioned in the text and figures are indicated. The Bruant Sandstone Fm. is not represented in this section. The northern part of the Voirons Flysch is mostly covered by Quaternary deposits and does not outcrop. Beyond the Allinges Hills, outcrops of the Voirons Flysch are rare and the eastern limit is not well constrained

rock bodies exposed in the Southern Alps (Sarasin 1894; Pilloud 1936; Lombard 1940; Cogulu 1961) such as the Bernina nappe, Canavese zone, Err-Albula granite and Falknis nappe. Later, based on petrographic and biostratigraphic data, Caron (1976) regrouped all these flyschs in a new tectonic unit, the Gurnigel nappe, which he correlated with the Sarine nappe (Upper Prealps nappe, Fig. 2) of South Penninic origin. Detrital grains were thought to originate from the Austro-alpine domain (Winkler 1983; Caron et al. 1989). The peculiar structural position of the Gurnigel nappe at the base of the Prealps nappe stack was then explained by the overthrusting of the Upper Prealps beyond the front of the Préalpes Médianes nappe, followed by out-of-sequence thrusting of the latter (Mosar 1991; Wissing and Pfiffner 2002). However, recent structural data from the Iberg Klippe (Trümpy 2006) and the younger age found by Ujetz (1996), Ospina-Ostios et al. (2013) and Ospina-Ostios (2017) now suggest that the Gurnigel flyschs could have been deposited in the Valais Ocean (Fig. 2), which would considerably simplify the kinematics of the Prealps.

Study area

The Voirons Massif, which comprises the western portion of the Gurnigel nappe, is located in the Chablais Prealps, at about 20 km from Geneva (Figs. 1, 3). It includes a series of smoothed hilltops, which are, in decreasing order of altitude, the Voirons (1480 m), the Grande Combe (1293 m), the Mont Vouan (978 m) and the Allinges Hills (754 m). The latter broadly constitute the eastern limit of the massif. The Voirons Massif is essentially made of flysch deposits (Lombard 1940; Jan du Chêne et al. 1975; Van Stuijvenberg 1980), whose stratigraphy has recently been revised (Ragusa 2015; Fig. 4). Accordingly, it now comprises four lithostratigraphic units:

1. The Voirons Sandstone Formation forms the crest and the eastern flank of the Voirons ridge (Fig. 4). It is a thick (200–300 m), sandstone-rich succession with variable amounts of intercalated marls (Fig. 5a, b). The base of the unit is marked by a marly succession with calcarenite beds (Fig. 5a) similar to the Hellstät Formation of the Gurnigel Flysch (Tercier 1928; Caron et al. 1980, 1989). Some m-thick conglomeratic layers are exposed along the Voirons crest. Described as "local deposits" by Lombard (1940), they include the pink granite lithoclasts (Fig. 6a) typical of the flyschs from the Gurnigel nappe (Caron 1976). The Voirons Sandstone Fm. presents a large range of sedimentary deposits from channel to lobe settings (Ragusa 2015). Deposition is constrained between the Middle Eocene and the Early Oligocene (planktonic foraminiferal zones P12 to P19, Ospina-Ostios 2013). The contact with the overlying Vouan Conglomerate Fm. is transitional (Ragusa 2015).
2. The Vouan Conglomerate Formation is exposed along the eastern flank of the Voirons ridge, and forms the neighbouring Mont Vouan (Fig. 4). It is a homogeneous stack (300–400 m thick) of coarse pebbly sandstones to matrix-supported conglomerates that are frequently amalgamated (Fig. 5c). They are mostly devoid of marly intervals, and include black sandstone and conglomerate lithoclasts of Paleozoic age (Fig. 6b). Pebbles and cobbles are also randomly distributed in sandy layers. Lateral variation and large scours (Frébourg 2006) characterise the Vouan Conglomerate Fm. which is restrained to channel depositional settings (Ragusa 2015). The scarce biostratigraphic data from this unit (Frébourg 2006; Ospina-Ostios et al. 2013; Ospina-Ostios 2017) suggest a Late Eocene–Early Oligocene age (planktonic foraminiferal zones P15 to P20). The contact with the Boëge Marl Fm. is sharp and does not present any tectonic deformation (Ragusa 2015; Ospina-Ostios 2017).
3. The Boëge Marl Formation (synonymous: Saxel Marl Fm.) was defined by Van Stuijvenberg and Jan du Chêne (1980) and comprises the Ludran Hills and the Grande Combe. It is one thick (>1000 m), predominantly marly succession, interspersed by cm-thick, sandstone-rich layers. The base is characterised by some dm-thick conglomeratic layers. The sandstone beds show frequent ripples and upper-plane bedding (Fig. 5d). The formation is affected by several tectonic folds and thrusts (Coppo 1999; Ragusa 2015; Ospina-Ostios 2017). This unit is interpreted as lobe or continental-slope deposits (Winkler 1984). The Boëge Marl Fm. shows a tectonic contact with the Préalpes Médianes nappe in the southern part of the studied area and a stratigraphic (?) contact with the overlying Bruant Sandstone Fm. in the Grande Combe area. Indeed, the progressive upward thickening of sandstone beds suggests a transitional contact. The Boëge Marl Fm. is of late Middle Eocene to Early Oligocene age (Ospina-Ostios et al. 2013; planktonic foraminiferal zones P13 to P20).
4. The Bruant Sandstone Formation (Ragusa 2015) consists of dm-thick, sandy beds interspersed by cm-thick, marly intervals. No conglomeratic intervals have been found in this formation, but its upper reaches comprise some microconglomerate layers. Its upper limit corresponds to the tectonic contact with the Préalpes Médianes nappe. From a petrographic viewpoint, the Bruant Sandstone Fm. is comparable to the Voirons Sandstone Fm., and is interpreted as channel to lobe deposits (Ragusa 2015). No biostratigraphic data have so far

Fig. 5 Main studied outcrops: **a** the Bons quarry (VS), **b** the lower Saxel quarry (*VSS*), **c** the Vachat millstone quarry (VC), **d** the Chauffemérande creek (BM), **e** the Grotte aux Loups (VC), **f** the Fenalet quarry (UH ?), **g** the Fayaux quarry (Fayaux-Pléiades Flysch) and **h** the Zollhaus quarry (Berra-Schwyberg Flysch). Location map is available in Figs. 1 and 3

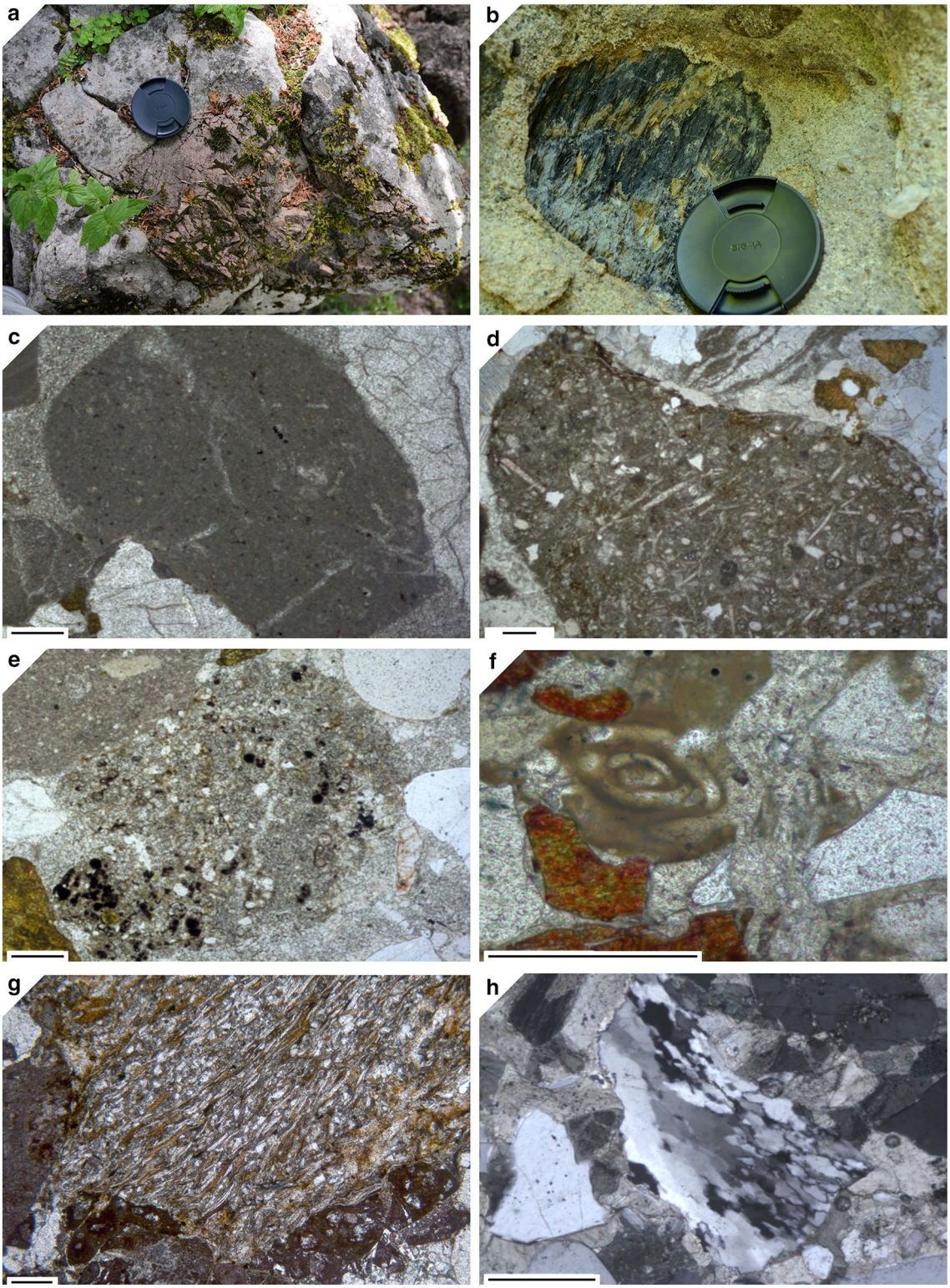

Fig. 6 Microphotography and macrophotography of typical grains found in the Voirons Flysch: **a** *pink* granite fragment, **b** *black* Paleozoic sandstone fragment, **c** mudstone fragments, **d** foraminifera and bioclastic wackestone fragment, **e** siliciclastic wackestone, bioturbation filling ?, **f** phosphatised foraminifera, **g** metamorphic clasts with micaceous lineations, and **h** tectonised quartz polycrystalline grains. The *black bar* represents 200 µm

been retrieved from this unit. The formation thickness is estimated at about 1000 m. Up to now, this unit was incorrectly interpreted as a sedimentary mélange (Kerrien et al. 1998) because of the pronounced (tectonic) deformation near the contact with the Préalpes Médianes nappe.

Methods

Sampling

A total amount of 278 sandstone samples were collected in about fifty outcrops of the Voirons Flysch. An additional exposure, the Fenalet quarry (Fig. 5f), to the East of the Allinges Hills, was also investigated, although it is generally attributed to the Ultrahelvetic because of its structural position and age (Gagnebin 1944; Badoux 1962, 1965, 1996). The Fayaux (Fig. 5g; Van Stuijvenberg et al. 1976) and the Zollhaus quarries (Fig. 5h; Bouma 1962; Crimes et al. 1981), that comprise respectively the Fayaux-Pléiades and the Berra flyschs, were also sampled for comparative purposes. Geographic location of the outcrops, stratigraphic logs and datasets are available on the GitHub page of the first author (https://github.com/jragusa/).

Thin section modal mineralogy

Counting was performed according to the Gazzi-Dickinson method (Dickinson and Suczek 1979; Ingersoll and Suczek 1979; Dickinson 1985). Grains were organised following the Zuffa classification (Zuffa 1980). 300 extrabasinal grains was counted per thin section using the ribbon method of Van der Plas (1962). Feldspar minerals were stained following the procedure developed by Norman (1974) and advices from Prof. Wilfried Winkler (ETH-Zürich). Using this technique, albite remains colourless but, in contrast to quartz grains, it is etched along the cleavage planes. Grains included in rock fragments (quartz, feldspars and micas) were counted separately (Critelli et al. 2007; Stefani et al. 2007; Das Gupta and Pickering 2008) and described according to the nomenclature of Weltje (2002) (–rv: volcanic rock, –rm: metamorphic rock, –rg: plutonic rock). Sand-size quartz and feldspars from igneous rock fragments are reported in their respective QAP ternary diagram (Quartz–Alkali feldspar–Plagioclase). By convention, we distinguished lithic fragments (i.e. polycrystalline grains with internal grain-size less than 63 µm) from rock fragments (internal grain-size coarser than 63 µm). Metamorphic lithic and rock fragments were determined following the colour guide of Garzanti and Vezzoli (2003). They are distributed between the low- (Rm1+), intermediate- (Rm3+) and high-metamorphic (Rm5+) grades, and described using the MI index (Metamorphic Index: Garzanti et al. 2004, 2010). Considering the sand-size limit, metamorphic grains of grade five were counted as rock fragments (Rm5). The status of mudstone and wackestone lithoclasts (Fig. 6c, d) is still questionable as there is no undisputable evidence for an extrabasinal origin (Zuffa 1980). They can be inherited from a sedimentary cover (extrabasinal origin) or reworked from a platform (intrabasinal origin; Critelli et al. 2007). In addition, the incorporation of calcareous grains in the counting is debated (Dickinson and Suczek 1979; Mack 1984). Calcareous grains are very sensitive to weathering and a small amount of terrestrial calcareous grains reaches marine basins (Arribas et al. 2000; Picard and McBride 2007). Considering that inclusion of detrital carbonate grains confers consistent provenance interpretation in some cases (Mack 1984), our results are presented without (continuous line) and with (dashed line) the micritic limestone clasts. In addition, grain counting includes also intrabasinal grains (authigenic and skeletal grains), cement and porosity.

Because formation boundaries are poorly defined in the Voirons Flysch (Van Stuijvenberg 1980; Van Stuijvenberg and Jan du Chêne 1980; Vial et al. 1989; Coppo 1999), the framework composition of samples was sorted independently of stratigraphic affiliation using a cluster analysis (Ward method and Euclidean distance; Fig. 7). Only grain classes exceeding 10% were selected (Qm, K, Lm, Qr, P, Ls, Lce, Qp, Lv and Lci; see Table 1 for description) to constrain the interpretation of the cluster tree, and limit the influence of minor grain classes. Each cluster defines a petrofacies which refers to similar compositional parameters (Dickinson and Rich 1972).

QEMSCAN® heavy-mineral analyses

Heavy-minerals were sampled from each petrofacies identified from the framework composition. They were extracted from fine- to medium-grained, well-preserved sandstones following Mange and Maurer (1992). The rocks were crushed and cement removed with acetic acid (10%) in a hot bath (70 °C). The 63–125 µm fraction of loose sediment was recovered by wet sieving. Dense minerals were separated using a liquor of sodium polytungstate (SPT) at $d = 2.90$ g/cm^3, and recovered by freezing the bottom part of centrifugation tube. Heavy- and light-mineral fractions were then dried and weighted. Finally, the heavy-mineral fraction was placed in moulds, consolidated with an epoxy resin, and subsequently polished to be analysed by an FEI QEMSCAN® Quanta 650F installed at the Department of Earth Sciences of the University of Geneva.

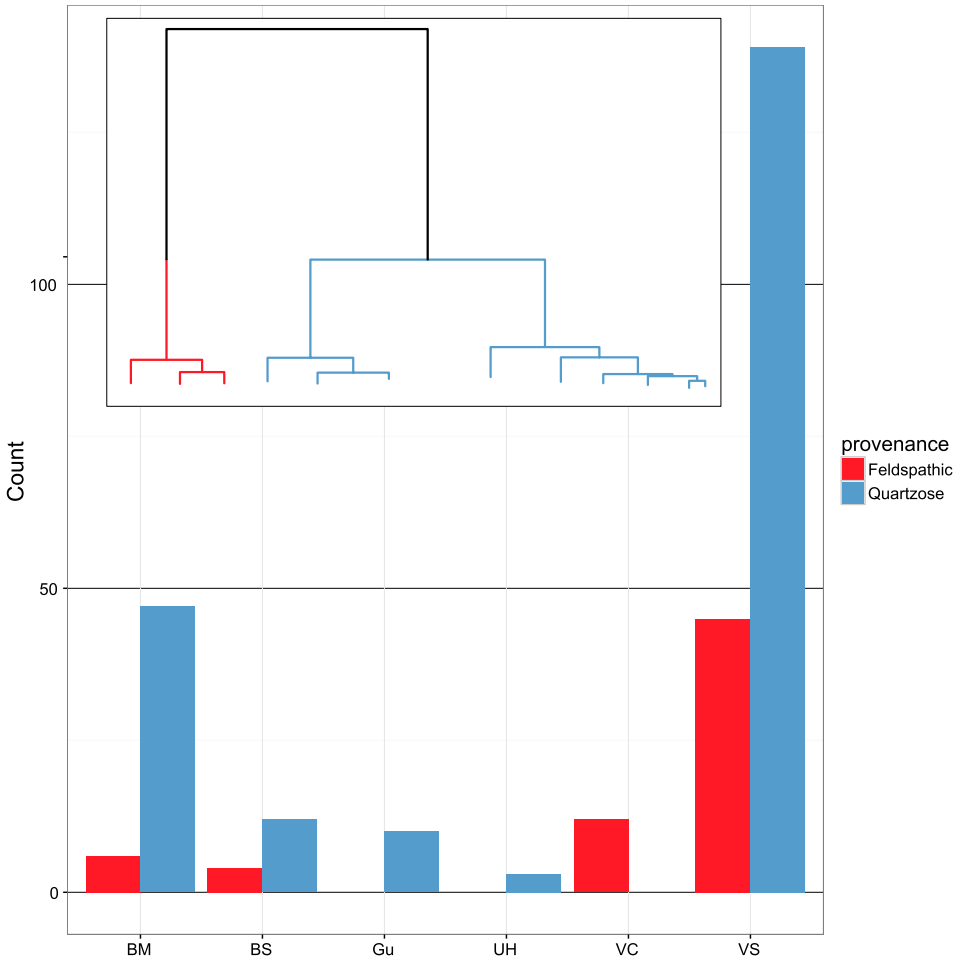

Fig. 7 **a** Relative proportion of the petrofacies within each stratigraphic unit. *AS* Allinges Sandstone, *BM* Boëge Marl Fm., *Gu* Other flyschs of the Gurnigel nappe, *UH* Fenalet quarry (Ultrahelvetic ?), *VC* Vouan Conglomerate Fm., *VS* Voirons Sandstone Fm. **b** Cluster tree diagram with the two identified petrofacies

The QEMSCAN mineral phase identification relied on the combination of back-scattered electron (BSE) contrast and EDS spectra giving information on the elemental composition (Gottlieb et al. 2000). Individual X-ray spectra were compared to a library of known spectra and a mineral name was assigned to each individual acquisition point. The X-ray EDS spectra library, initially provided by the manufacturer, has been further developed in-house using a variety of natural standards. Measurements were performed on carbon-coated plugs that were adequately polished. Analytical conditions included a high vacuum and an acceleration voltage of 25 kV with probe current of 10 nA. The X-ray acquisition time was 10 ms per pixel using a point-spacing of 5 µm. Up to 122 individual fields of view were measured in each sample, with 1.5 mm per single field. QEMSCAN® data processing (e.g. unknown spectra debugging, particle boundary disambiguates, field stitching) was performed using the FEI iDiscover software. Composite mineral entries like garnet and tourmaline were defined by their respective EDS spectra consisted of individual elemental peak. Their intensities are defined by the ratios of measured elemental peaks and theoretical peaks representing a single pure compounds matter solely consisted of the element in question. Henceforth, the garnet entry comprises a comprehensive chemistry covering most of garnet species. Such a mean composition is defined by the following peak intensities: 35–200 (oxygen), 50–140 (aluminium), 80–210 (silicon), 20–210 (iron), 0–140 (magnesium), 0–100 (calcium) and Al/Si ratio that exceeded 0.3. Following the analogue reasoning, the tourmaline composition used in this research consisted of oxygen (variable intensities), aluminium (140–280), silicon (120–220), sodium (0–45), magnesium (0–104), calcium (0–38), and iron (0–200), whereas fluorine and carbon may be encountered in EDS spectrum fitting the tourmaline entry compositional criteria.

Garnet grains are organised into six different classes including melting phases: almandine, almandine-pyrope, almandine-pyrope-grossular, almandine-spessartine, grossular and undetermined garnets. Tourmaline grains are grouped into schorl, dravite and undetermined tourmaline. For each mineral group, the elemental composition of ten grains is extracted within each class and for each sample.

Table 1 Additional key indices for the framework composition and heavy-minerals

Key indices	Definition
Framework composition	
Qm = Qms + Qr	Total monocrystalline quartz
Qp = Qps + QpT	Total polycrystalline quartz
Qr = Qrg + Qrv + Qrm	Quartz in rock fragments
Kr = Krg + Krv + Krm	K-feldspar in rock fragments
K = Ks + Kr	Total K-feldspars
Pr = Prg + Prv + Prm	Plagioclase in rock fragments
P = Ps + Pr	Total plagioclases
Lc = Lci + Lce	Total calcareous lithic
Lt = L + Qp	Total lithics
D = Ap + Grt + Hb + Rt + St + Zr	Dense minerals
M = Bt + Mu	Total micas
MI = Rm1/Rm × 100 + Rm2/Rm × 200 + Rm3/Rm × 300 + Rm4/Rm × 400 + Rm5/Rm × 500	Metamorphic index (Garzanti et al. 2004)
Zuffa classification	
NCE = Q + F + L + D + M	Non-carbonate extrabasinal grains
NCI = Glt + FeO + P + Fph	Non-carbonate intrabasinal grains
CE = Lce	Extrabasinal calcareous grains
CI = Lci + Bc	Intrabasinal calcareous grains
Heavy-mineral	
LgM = Ep + Chl	Low-grade metamorphic heavy-minerals (Garzanti et al. 2004)
HgM = St + And + Ky + Sil	High-grade metamorphic heavy-minerals (Garzanti et al. 2004)

Mineral abbreviations are based on the compilation of Whitney and Evans (2010) excepted: *Qms* single monocrystalline quartz, *Qps* non-tectonised polycrystalline quartz, *QpT* tectonised polycrystalline quartz, *Ks* single K-feldspar, *Ps* single plagioclase

In addition, 595 and 255 representative grains of garnet and tourmaline respectively were analysed by SEM-EDS system using an FEI QEMSCAN® Quanta 650F installed at the Department of Earth Sciences of the University of Geneva that was operated in the scanning electron microscope mode. The Bruker ESPRIT software was used for EDS spectra quantification in a standardless mode. Thereafter, garnet and tourmaline phase chemistry served as a basis to calculate the proportions of end members of respective minerals using the spreadsheets designed by Andy Tindle from the Open University of Buckinghamshire for garnet (http://www.open.ac.uk/earth-research/tindle/AGTWebPages/AGTSoft.html).

The heavy-mineral content (HMC) and transparent heavy-mineral content (tHMC) indices of Garzanti and Andò (2007) provide the heavy-mineral content in sandstone. They are based on the improved estimation of the H index of Baker (1962). A preliminary single garnet grain analysis was performed by QEMSCAN®. The different species of the garnet supergroup (Grew et al. 2013) detected by QEMSCAN® are constrained to the most abundant species, the transitional solid solution members and an undetermined group which gathers all the species are not documented in QEMSCAN® database.

Thin section heavy-mineral counting

Ten heavy-mineral fractions (63–400 µm) from Ragusa (2009) were also recounted (Table 3). The protocol extraction is similar to those of the QEMSCAN® analysis, apart of the use of bromoform ($d = 2.89$ g/cm^3) and the recovering by filtration. Thereupon, heavy-mineral fractions were dried and placed on thin section. Total amount of 200 transparent heavy-mineral grains was counted.

Data processing

Mineral abbreviations are based on the compilation of Whitney and Evans (2010) with a few exceptions like limonite (=Lim) to avoid confusion with metamorphic lithics (Lm). Additional grains are reported in Table 1. Computations and statistical analysis were performed using the R software (R Core Team 2015). Samples distribution in a ternary diagram (Figs. 9, 11, 17, 19) is associated with fields indicating 90% confidence regions for the distribution, calculated via Mahalanobis distance and log-ratio transformation (Hamilton 2016), which is more accurate and reliable (Weltje 2002) than a hexagonal confidence

area (Ingersoll 1978). QEMSCAN® results were treated in FEI iDiscovery software v.5.2.

Results

Voirons Flysch framework composition

The dataset of the modal mineralogy of the Voirons Flysch is attached in supplementary data (Table A1). It describes raw data and stratigraphic affiliation for each sample. Samples are composed of poorly to well-cemented sandstones (Fig. 8). Sandstone beds mostly contain non-carbonate extrabasinal grains (NCE, 27.0–97.5%), minor carbonate intrabasinal grains (CI 0–11.13%) and non-carbonate intrabasinal grains (NCI, 0–18.54%). Cl grains comprise a typical heterozoan assemblage including, in decreasing order, red-algae, foraminifers (e.g. nummulitids, discocyclinids, planktonic foraminifera), bryozoan and echinoid fragments, whereas the NCI grains consist of glauconite, phosphates (single grains and recrystallised foraminifers, Fig. 6e) and of some opaque minerals. Mudstone to wackestone lithoclasts were incorporated into the CI class, and consequently the proportion of carbonate extrabasinal (CE) grains is very low (<2.5%). Calcite cement mostly fills up interstitial voids (0–63.3%) and porosity is usually very low, but may reach up to 25.6% in few cases.

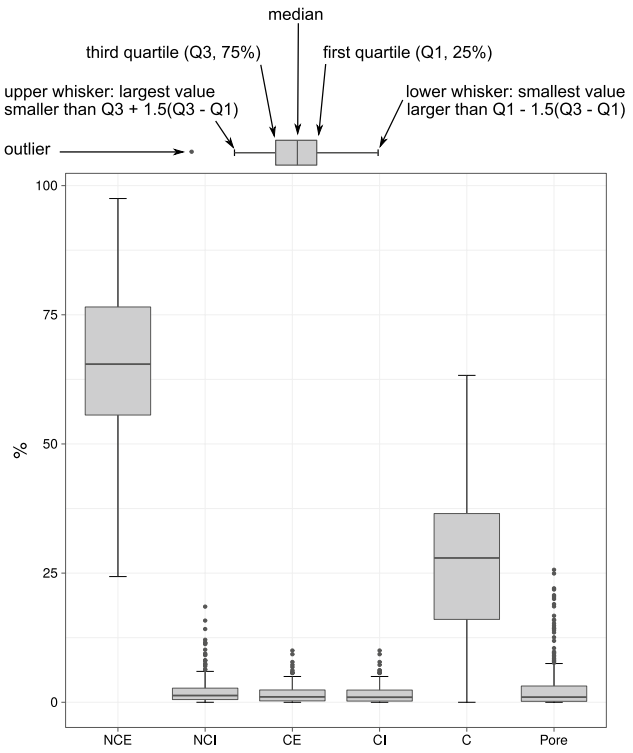

Fig. 8 Box-whisker plot of the main grain classes of Zuffa (1980)

Cluster analysis on framework composition identifies two branches of different importance (Fig. 7). Based on their framework composition, the right branch (75.90% of the samples) is determined as a Quartzose petrofacies, whereas the left branch (24.10% of the samples) corresponds to a Feldspathic petrofacies. The Quartzose and Feldspathic petrofacies are mainly identified by distinctive Qm/F ratio (Figs. 9, 10) with a slight overlap of the confidence areas. The incorporation of polycrystalline quartz (Qp) into the Q pole of the QFL diagram (Fig. 9a) emphasises their important proportion, flattening the scatter plot along the Q–F axis.

The Quartzose petrofacies

The Quartzose petrofacies presents a high Q/F ratio (Fig. 10). The incorporation of mudstone to wackestone lithoclasts in the counting, especially in the QFL ternary diagram (Fig. 9a), reduces the strong influence of polycrystalline quartz in the samples of the Quartzose petrofacies. Considering the low lithic content and regarding the overall composition, the relative contribution of these micritic grains is low (Lc/QFL ratio, Fig. 10), which

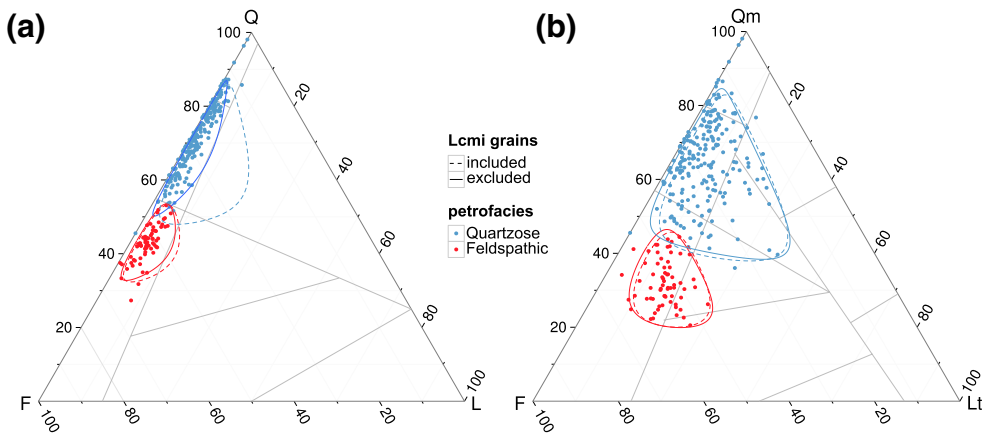

Fig. 9 Petrofacies distribution in the QFL and QmFLt ternary diagrams of the Dickinson model

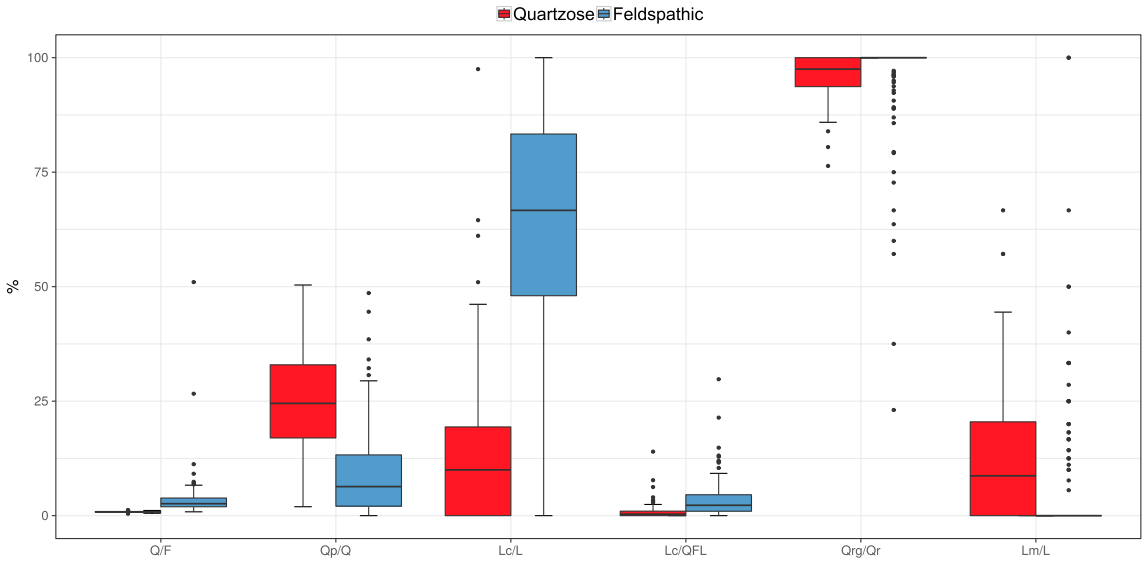

Fig. 10 Box-whisker plot of the main ratio for the framework composition. For key to box plots see Fig. 8

explains the similar distribution in the QmFLt ternary diagram (Fig. 9b).

The distribution of monocrystalline grains (Fig. 11a) shows a Qm–KP trend without a clear distinction within feldspars. The sample distribution is similar to that on QFL and QmFLt diagrams (Fig. 9), emphasising the strong influence of the Q/F ratio in the petrofacies. The distribution of quartz is shown in the ternary diagram QmsQpQr (Fig. 11b). Samples are concentrated around the Qm pole drawing a trend toward the Qr pole. The latter is mostly represented by a granitic source (Qrg/Qr ratio, Fig. 10) The Quartzose petrofacies is mature with a high proportion of monocrystalline quartz. The proportion of polycrystalline quartz is very low (Qp/Q ratio, Fig. 10), and the discrimination of the provenance is not as pronounced as in QFL (Fig. 9) and QpLsmLvm ternary diagrams (Fig. 11a). The composition of feldspar grains ranges from orthoclase to anorthite with a low albite content (Fig. 11c). However, a slight increase in the albite content, together with the alkali-feldspars, can be explained by the relative depletion of calcium plagioclase by albitisation, as already pointed out by Morad et al. (1990). Single grains represent the most abundant feldspars grains (Fig. 11d, e).

Several samples of the Quartzose petrofacies are devoid of lithic grains, and thus cannot be used in the analyses ($L=0$, Fig. 10). The distribution of lithic fragments identifies a magmato-sedimentary assemblage (Fig. 11d). However, the lithic grains are subordinate to the high content of polycrystalline quartz, as illustrated in the QpLsmLvm ternary diagram (Fig. 11e).

The inclusion of mudstone to wackestone grains confers a more sedimentary-rich composition to the Quartzose petrofacies (Lc/L, Fig. 10). Sedimentary clasts are mostly represented by intrabasinal micritic limestone grains (Lcmi) presenting a large spectrum of textures from mudstones (Fig. 6c) to foraminifer- and bioclast-rich wackestones (Fig. 6d). The grain shapes are variable, from rounded to angular. Some micritic grains presenting a fuzzy boundary and containing quartz and glauconite (Fig. 6e) could possibly correspond to the filling of bioturbations. The lack of oxidised contours or other post-sedimentary weathering features (Zuffa 1980) precludes an extrabasinal origin for these grains which are included in the CI grains as rip-up clasts reworked from the platform (Garzanti 1991). Others sedimentary grains include chert debris, silt-size argillaceous fragments, and very rare recrystallised limestone clasts. The chemical and mechanical stability of chert fragments facilitates their persistence in the sedimentary record, which leads to overestimate their relative content. They could be an indicator of carbonate source rocks (Mack 1984). Clayey to silty fragments are undoubtedly extrabasinal, but do not provide any information about their respective source. Sandstone fragments are usually absent as they directly provide single grains (e.g. quartz, feldspars). By contrast, conglomerate fragments were found in the conglomerate layers. Amber grains have been reported in the Allinges Sandstone (de Mortillet 1863; Renevier 1893) and in the Vouan Conglomerate Fm. (Pilloud 1936). Sparse phosphate grains and phosphatised foraminifers are also found (Fig. 6g), especially in the Boëge Marl Fm. No trend can be deduced from the sedimentary clasts as their distribution varies strongly through the samples. The relative content of the CE grains in sandstone samples is very low (Fig. 8), which contrasts to their widespread occurrence in conglomerates (Cogulu 1961; Winkler 1983;

Frébourg 2006). This may result either from (1) preferential dissolution, (2) late incorporation in the sedimentary process or (3) dilution by comparatively better-preserved igneous rocks.

Magmatic clasts are both of plutonic and volcanic origin. Most of the examined grains are plutonic rock fragments (Fig. 11f), and plot in the granite to granodiorite fields, extending up to the tonalite field in some samples. Some microgranites were also encountered. The low proportion of volcanic grains precludes a reliable identification of volcanic-rock fragments. Samples plot in the quartz-andesite to rhyolite fields (Fig. 11g), and andesitic lithoclasts have been reported in thin sections (Ospina-Ostios et al. 2013).

The Quartzose petrofacies is usually devoid of metamorphic grains (Lm/L ratio, Fig. 10). Thus, few points are plotted inside the ternary diagrams (Fig. 11h). They are concentrated near the end members or along the axis due to their scarcity. However, considering the mean values, the Quartzose petrofacies is preferentially located near the Rm5 + end member (High metamorphic grade). The Metamorphic index is low (Figs. 10, 11i), and the Quartzose petrofacies presents also a low amount of tectonised polycrystalline quartz (Figs. 10, 11j) which is typical of remnant oceanic deposits off- scraped at shallow levels (Garzanti et al. 2010).

The Feldspathic petrofacies

The Feldspathic petrofacies presents a low Q/F ratio (Fig. 10). Samples are not affected by the counting of mudstone to wackestone fragments (Fig. 8), which emphasises the scarcity of these grains in this provenance (Lc/L ratio, Fig. 10).

The Feldspathic petrofacies shows a high content in plagioclase among monocrystalline grains (Fig. 11a). Some albitisation of plagioclase (Morad et al. 2000) is also observed as suggested by the minor content in albite (Fig. 11c). Quartz grains comprise an elevated content in lithic quartz grains (Fig. 11b, Qr) and polycrystalline quartz (Qp/Q ratio, Fig. 10). The latter usually originates from granitic rock fragments (Qrg/Qr ratio, Fig. 10), but gneisses cannot be excluded as an alternative source of polycrystalline quartz.

The Feldspathic petrofacies always contains a significant fraction of lithic fragments (Fig. 11d, e) including a large proportion of metamorphic lithoclasts (Lm/L ratio, Fig. 10), in addition to the magmato-sedimentary assemblage. However, the lithic grains are less abundant than the polycrystalline quartz (Fig. 11e), and the confidence areas present a large overlap with the Quartzose petrofacies (Fig. 11d, e).

The magmatic lithic content is relatively similar to that described in the Quartzose petrofacies (Fig. 11f, g). Sample distribution overlaps the Quartzose petrofacies in the plutonic rocks (Fig. 11f). More volcanic rocks are observed in the Feldspathic petrofacies and plot in the Rhyodacite to Quartz-andesite fields (Fig. 11d). The Feldspathic petrofacies is characterised by significant inputs in metamorphic rock fragments (Lm/L ratio, Fig. 10) and a high MI index (Figs. 10, 11i) dominated by high-grade, with subordinate low-grade, metamorphic lithics (Fig. 11i, j). However, such a high MI value is not common in remnant-ocean deposits off-scraped at shallow depth (Garzanti et al. 2010; Fig. 8). Protoliths likely consist of sedimentary rocks according to the nomenclature of Garzanti and Vezzoli (2003). Tectonised polycrystalline quartz (QpT) stands for a reliable indicator of the supply of metamorphic rock fragments (Young 1976; Figs. 10, 11j). The metamorphic clasts, especially schists, are more easily crushed during the sediment transport (Picard and McBride 2007).

Voirons Flysch heavy-mineral assemblage

The dataset of the heavy-minerals of the Voirons Flysch is summarised in Tables 2 and 3 for the QEMSCAN® analyses and the samples from Ragusa (2009), respectively. The abundance of heavy-minerals and transparent heavy-minerals (HMC and tHMC) in the 63–125 µm fraction is poor to moderately poor (sensu Garzanti et al. 2010) in both petrofacies (Fig. 12; Table 2). The small gap between HMC and tHMC indices illustrates an elevated content of transparent heavy-minerals (tHM). The assemblage of tHM represents 60–90% of the dense minerals followed by opaque grains and micas (Ragusa 2015). The lowest content in tHM is found in the distal density–current deposits (JR5 and JR57), and is associated with a higher mica content (Fig. 13). In both grain-size ranges, transparent heavy-minerals are represented by ultrastable (ZTR group) and stable (garnet and apatite) species in both petrofacies (Fig. 14). Accessory grains of the tHM trace group consist of unstable minerals (e.g. barite, epidote, pyroxene and hornblende).

There is some discrepancies between the both fractions. The main difference lies in the relative distribution of the mineral species (e.g. higher zircon and lower rutile content in the 63–400 µm). Rutile and titanite are relatively more abundant in the 63–125 µm fraction than staurolite, tourmaline and zircon and inversely in the 63–400 µm fraction. These differences may derive from inherited grain-size in source rocks (Morton and Hallsworth 1999). In addition, the QEMSCAN® determination may also influence the relative proportion with a better identification of the finest fraction which is more difficult to constrain with an optical microscope. Despite these discrepancies, the relative abundance of some diagnostic species (e.g. garnet), or dedicated ratios discriminate Quartzose and Feldspathic petrofacies in both grain-size ranges (Figs. 12, 14).

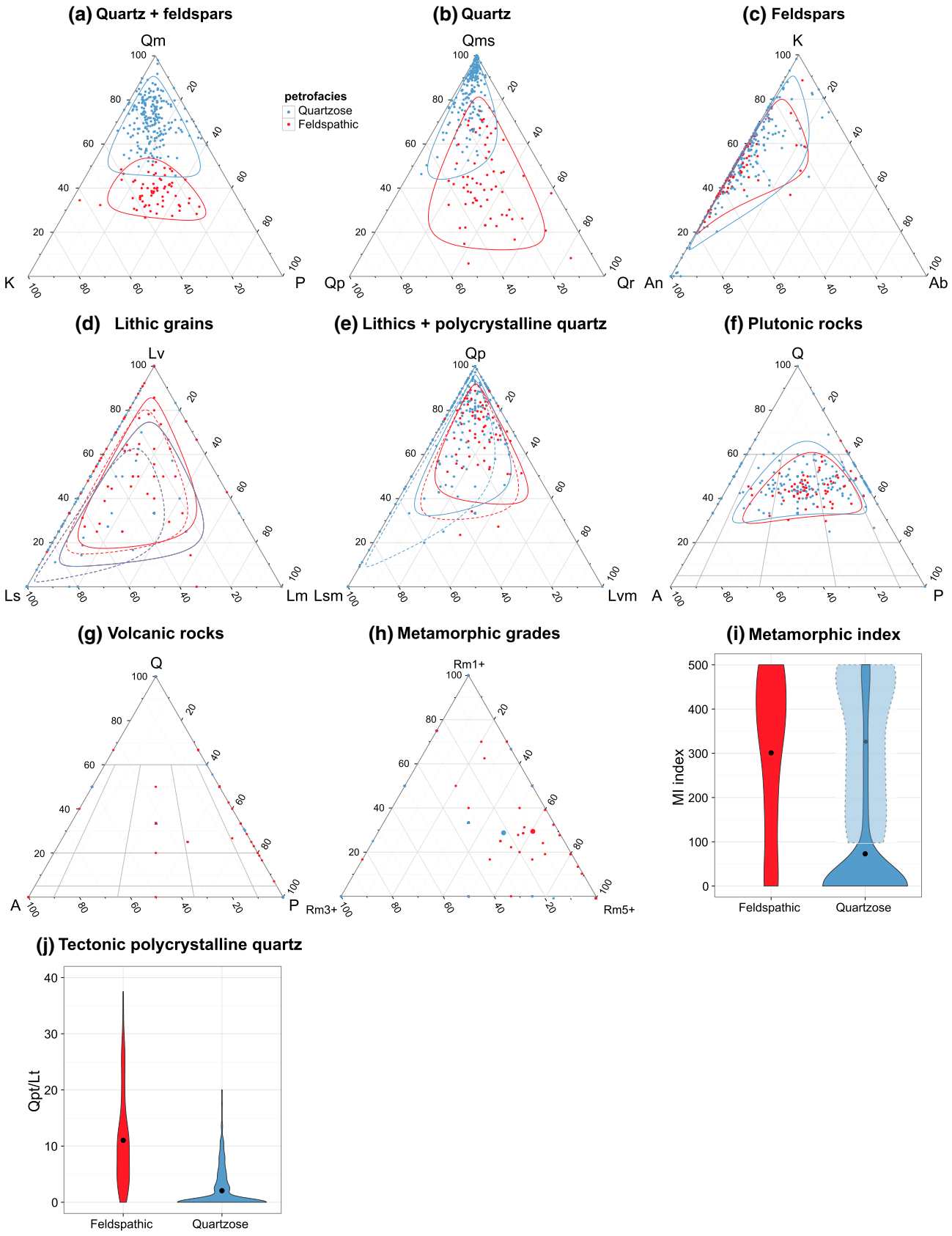

◂**Fig. 11** Monocrystalline grain distribution illustrated with overall composition (**a**) and dedicated distribution of quartz (**b**) and feldspars (**c**–**e**). Polycrystalline grain distribution illustrated with overall composition (**f, g**), estimated composition of plutonic (**h**), volcanic rocks (**i**) and metamorphic grades of Garzanti et al. (2004) (**j**). Metamorphic inputs are also evaluated with the MI index (Garzanti et al. 2004, 2010) (**k**) and the relative content of tectonic polycrystalline quartz (**l**)

The Quartzose petrofacies

The Quartzose petrofacies essentially contains abundant tourmaline reflected by lower ATi (Morton and Hallsworth 1994) and higher ZTR indices (Fig. 12; Table 2). The garnet content is low, as emphasised by the low GZi index (Fig. 12; Table 2; Morton and Hallsworth 1994). The scarce K-rich volcanic glass confirms the rhyolitic source described in Fig. 11g. A large variation in mica distribution and the occurrence of biotite characterise the Quartzose petrofacies.

Preliminary single-grain analysis on garnets identified almandine and almandine–pyrope solid solution (mean = 86.09%) as dominant phases (Fig. 15a). Subordinate grains are almandine–pyrope–grossular and almandine-spessartine solid solutions (mean = 6.95%). Less than 10% of garnets grains were undetermined. Moreover, the Quartzose petrofacies shows the schorl-dominated assemblage among tourmaline grains (Fig. 16).

The Feldspathic petrofacies

The Feldspathic petrofacies is characterised by a high content in garnet and an elevated GZi index in the 63–125 µm fraction (Fig. 12; Table 2). Consequently, the ATi index is high and the ZTR index is low (Fig. 12; Table 2). The distribution of micas is relatively constant in the Feldspathic petrofacies and is dominated by chlorite (Fig. 13).

Single grain analysis on garnet identified almandine-pyrope-grossular and almandine-spessartine solid solutions, similar to the assemblages found in the Quartzose petrofacies. As for the latter, the tourmaline assemblage is dominated by schorl (Fig. 16).

Garnet and tourmaline geochemistry

The geochemical data of garnet and tourmaline are summarised in supplementary data (Tables A3 and A4, respectively). Both petrofacies share similar garnet distribution dominated by almandine (Alm) and almandine–pyrope (Alm–Prp) varieties (Fig. 15a). The relative composition of each class is summarised in Fig. 15c. Several classes contains a minor amount of andradite. The almandine–spessartine phase (Alm-Sps) includes a minor content in grossular. Undetermined garnets correspond to spessartine–almandine–grossular (Sps-Alm-Grs). Finally grossular (Grs) is relatively pure (>80%) with few amount of andradite. Almandine–pyrope–grossular (Alp–Prp–Grs) is also reported in trace amount.

Both petrofacies contain also a similar tourmaline composition dominated by schorl (Srl) and secondary dravite (Drv) (Fig. 16). Undetermined tourmaline identified by the QEMSCAN® correspond to Drv-rich Srl. Tourmaline geochemistry shows a wide compositional variation governed by Fe content.

Discussion

Petrofacies distribution in the stratigraphic subdivisions of the Voirons Flysch

As mentioned previously, the stratigraphic units of the Voirons Flysch were up to now poorly differentiated from a petrographic viewpoint (Lombard 1940; Van Stuijvenberg 1980; Charollais et al. 1998). Our modal composition analysis demonstrates that the Vouan Conglomerate Fm. is restricted to the left branch of the cluster tree (Fig. 7), and shows a homogeneous composition (Fig. 9). It thus represents the most typical stratigraphic unit of the Feldspathic petrofacies. However, several samples from other formations, especially from the Voirons Sandstone Fm., are located on the same branch as the Vouan Conglomerate Fm. (Fig. 7). The feldspatho-quartzo-lithic composition of these samples strongly differs from the other samples of these formations, and rather corresponds to the Vouan Conglomerate Fm. They consist of single beds, randomly distributed in the Voirons Sandstone Fm., in the Boëge Marl Fm. and in the Bruant Sandstone Fm. (Fig. 17). They are numerous near the boundary between the Voirons Sandstone Fm. and the Vouan Conglomerate Fm. which suggests an interfingering rather than a tectonic contact between these two units (Fig. 17).

The other lithostratigraphic units of the Voirons Flysch are characterised by the Quartzose petrofacies (Fig. 7). The latter represents the major source of detritus of the Voirons Flysch, and presents a wide spectrum of composition controlled by the depositional settings in a deep-sea fan (Ragusa 2015). The Quartzose petrofacies of the crest conglomerates (e.g. "Conglomérat de Pralaire"; Lombard 1940; Fig. 4) precludes an affiliation with the Vouan Conglomerate Fm., as stated by Van Stuijvenberg (1980).

It is impossible to recognise the provenances from the observation of sandstone beds in the field, unless they are interstratified with conglomerate layers comprising typical lithoclasts (e.g. pink granite fragments for the Quartzose petrofacies and black sandstone clasts of Paleozoic age for the Feldspathic petrofacies). Hence, the localisation of the Feldspathic petrofacies in single beds of the Voirons Flysch

Table 2 Heavy-mineral raw data from 63 to 125 µm fraction analysed on QEMSCAN®

Sample	Location	Petrofacies	HMC	tHMC	Ap	Mz	Chl	FeO	Grt undet	Alm	Grs	Alm-Prp	Alm-Prp-Grs	Bt	Ms	Rt	St	Ttn	Tur undet	Drv	Srl	Zrn	&tHM	Opaque	Other	Undet	Total
JR20	Upper Saxel quarry	Feldspathic	1.715	1.389	9617	579	3832	3384	96	724	32	3228	25	3823	938	6375	25	3864	244	1	243	1535	32	6025	4826	229	39,481
JR21	Upper Saxel quarry	Feldspathic	1.127	0.873	7931	542	1708	10,214	99	1635	7	2235	96	1104	1241	6395	94	1177	529	3	526	1311	33	255	9790	344	38,796
JR273	Fillignes 2 quarry	Quartzose	0.795	0.574	4355	193	972	2703	16	202	0	592	5	1203	1168	2426	129	544	759	13	746	713	18	4881	6273	233	23,596
JR278	Chez le Merizier stream	Quartzose	0.807	0.596	4409	412	525	4242	36	499	0	1062	27	1001	426	9497	258	1619	2815	21	2794	1658	48	7275	4696	266	38,765
JR329	Allinges Castle quarry	Quartzose	0.650	0.594	2866	368	648	2258	37	295	0	626	23	560	801	5401	66	2511	1797	20	1777	1205	26	543	12,346	108	31,048
JR330	Allinges Castle quarry	Quartzose	0.457	0.343	4596	644	605	8027	57	968	0	786	46	656	447	7028	83	1082	2440	16	2424	2031	57	850	5014	168	32,785
JR331	La Molertaz stream	Feldspathic	0.474	0.332	4246	442	1405	14,467	85	5584	14	2234	3	807	938	8919	80	2535	391	13	378	1513	56	118	4496	99	44,135
JR341	Allinges Castle path	Quartzose	0.483	0.368	4369	827	114	7877	39	414	0	218	14	985	247	4113	69	723	6674	23	6651	1805	30	62	4624	31	34,713
JR347	La Molertaz stream	Feldspathic	0.805	0.650	5387	793	1400	5609	61	1377	0	2183	25	744	576	11,429	360	2363	1360	15	1345	2052	68	2595	4025	196	37,783
JR349	La Janière	Quartzose	0.929	0.823	6517	840	129	3830	40	181	0	144	13	139	86	9205	324	2928	3137	28	3109	4804	133	28	1462	103	29,823
JR352	Combe Ecuer stream	Quartzose	0.718	0.415	7180	769	87	5577	30	312	1	140	11	446	299	7361	590	2166	2101	15	2086	1309	153	1942	1737	143	26,506
JR353	Combe Ecuer stream	Quartzose	0.805	0.618	5870	1046	679	5676	68	699	15	749	36	1590	1114	7695	684	824	2955	14	2941	2148	112	7079	5680	553	41,311
JR370	Chauffemérande stream	Quartzose	0.692	0.536	1646	273	283	7013	323	495	8	701	20	1491	389	2342	95	2984	974	7	967	1253	31	1443	13,752	338	34,909
JR375	Grotte au Loups	Feldspathic	0.863	0.679	3647	246	2393	9087	34	6438	0	3725	15	2131	1759	6269	5	1102	269	16	253	594	57	109	5089	142	39,487
JR376	Fenalet quarry	Quartzose	0.728	0.521	8483	239	208	328	4	7	0	847	0	795	348	8019	0	525	1470	24	1446	1281	139	4073	11,035	451	31,000
JR5	Bons quarry	Quartzose	0.417	0.346	2960	179	1069	4795	34	140	3	1112	20	7449	356	3138	66	1130	591	17	574	623	35	1003	9055	745	31,955

Table 2 continued

Sample	Location	Petrofacies	HMC	tHMC	Ap	Mz	Chl	FeO	Grt undet	Alm	Grs	Alm-Prp	Alm-Prp-Grs	Bt	Ms	Rt	St	Ttn	Tur undet	Drv	Srl	Zrn	&tHM	Opaque	Other	Undet	Total
JR57	Saxel stream	Quartzose	1.357	1.035	2298	155	3374	9321	156	3974	0	3031	25	6785	939	3351	399	1645	903	10	893	767	158	701	3827	377	040636
JR75	Supersaxel road	Quartzose	1.277	1.129	1817	320	283	5696	58	1006	1	628	31	211	196	2886	217	4192	1463	7	1456	1577	34	7347	2036	63	29,388

Mineral abbreviations are based on the compilation of Whitney and Evans (2010). *Ap* apatite, *Mz* monazite, *Chl* chlorite, *FeO* iron oxides, *Grt undet* undetermined garnet, *Alm* almandine, *Grs* grossular, *Alm-Prp* almandine-pyrope solid solution, *Apl-Prp-Grs* almandine-pyrope-grossular solid solution, *Bt* biotite, *Ms* muscovite, *Rt* rutile, *St* staurolite, *Ttn* titanite, *Tur undet* undetermined tourmaline, *Drv* dravite, *Srl* Schorl, *Zrn* zircon, *&tHM* other transparent heavy-mineral (hornblende, pyroxene, serpentinite, spinel and talc), *Opaque* opaque grains (pyrite, other oxides), *Other* non-heavy-minerals (feldspar, kaolinite, quartz and rhyolitic volcanic glass), *Undet* undetermined grains

and the fine-tuning of the boundaries of the Vouan Conglomerate Fm. remains problematic. In addition, these new data modify the stratigraphic affiliations of some outcrops (Ragusa 2015). In particular, the framework composition of the deposits exposed in the Fenalet quarry indicates that they must be correlated with the Voirons Flysch, and not with the Ultrahelvetic units.

Provenance of the Quartzose petrofacies

The quartz-rich composition and low HMC values of the Quartzose petrofacies correspond to the transitional continental to mixed tectonic settings (Fig. 9) of the Dickinson model (Dickinson 1985; Dickinson and Suczek 1979). Rock composition describes a low unroofed basement source including crystalline rocks and a sedimentary cover. The occurrences of zircon, tourmaline, xenotime, and monazite are common in intermediate to acidic granite and their metamorphic counterparts as well as in polycyclic detrital sandstones (Fig. 14; Mange and Maurer 1992; Stefani et al. 2007; von Eynatten and Dunkl 2012). Tonalite composition is confirmed by the high ATi index (Fig. 12; Bütler et al. 2011) and the negative correlation of apatite with silicates (von Eynatten and Dunkl 2012). Occurrence of andesite grains has also been reported (Ospina-Ostios et al. 2013). Tourmaline grains plots in fields 2, 3, 4 and 5 of the ternary discrimination diagram (Henry and Guidotti 1985; Fig. 16b), suggesting a wide range of source rocks. The latter include igneous rocks (fields 2 and 3) and metasedimentary rocks (fields 4 to 6) (Henry and Guidotti 1985; Mange and Maurer 1992). In addition, the minor amount of dravite further suggests igneous rocks as the main source of tourmaline (Fig. 16a). Sedimentary inputs have probably been underestimated, and might contribute a lot to the detrital sedimentation (Picard and McBride 2007). The ZTR index suggests an important reworking of detrital sedimentary rocks (Fig. 12). Sedimentary clasts found in conglomerate layers originate from a carbonate-rich stratigraphic succession of Triassic to Cretaceous age (Ragusa 2015). Further analyses are needed to better constrain the source of some peculiar facies (e.g. neritic carbonates similar to Urgonian Limestones; Lombard 1940). Likewise, the widespread occurrence of phosphate in the Tethyan realm from the Cretaceous to the Eocene (Broudoux 1985; Notholt et al. 1989; Föllmi 1990) is not a reliable indicator of a palaeogeographic origin. Amber grains are also found in other locations of the Gurnigel nappe (Tercier 1928), and correspond to a fluvial or coastal source. They do not relate to a particular palaeogeographic origin.

Our petrographic data (quartz-rich assemblage, high ZTR index) further suggest that the Quartzose petrofacies is very mature, and experienced polycyclic sedimentation, as confirmed by its location in the mixed field of the

Table 3 Recounted heavy-mineral raw data from 63 to 400 µm fraction from Ragusa (2009)

Sample	Location	Petrofacies	HMC	tHMC	Ap	Chl	Grt	Bt	Ms	Rt	St	Ttn	Tur	Zrn	&tHM	Opaque	Other	Total
F2a	Fillinges quarry	Quartzose	0.367	0.125	89	5	7	32	1	16	10	12	20	50	2	541	80	829
F2b	Fillinges quarry	Quartzose	0.353	0.135	30	19	10	43	2	9	6	7	43	50	1	520	82	788
F3b	Fillinges quarry	Quartzose	0.238	0.154	43	67	14	70	1	31	13	2	9	65	0	524	52	848
M1	Molière grind quarry	Feldspathic	0.169	0.130	36	9	23	19	3	10	3	5	4	11	0	34	20	174
M3	Molière grind quarry	Feldspathic	0.370	0.297	38	9	50	36	2	36	14	1	23	78	0	310	51	636
Sa1	Moutonnières	Feldspathic	0.202	0.142	15	24	27	49	11	12	9	0	5	11	1	104	44	293
Sa2	Moutonnières	Feldspathic	0.478	0.166	22	0	21	27	2	12	16	2	20	29	0	84	114	307
Sa3	Moutonnières	Quartzose	0.264	0.121	41	4	6	10	2	16	15	2	54	48	0	75	116	323
Sa4	Moutonnières	Quartzose	0.302	0.155	16	13	8	19	3	13	10	7	7	36	0	65	53	220
Sa6	Moutonnières	Quartzose	0.238	0.173	17	0	21	12	0	21	26	0	39	97	0	323	53	595

Mineral abbreviations are based on the compilation of Whitney and Evans (2010) and similar to Table 2

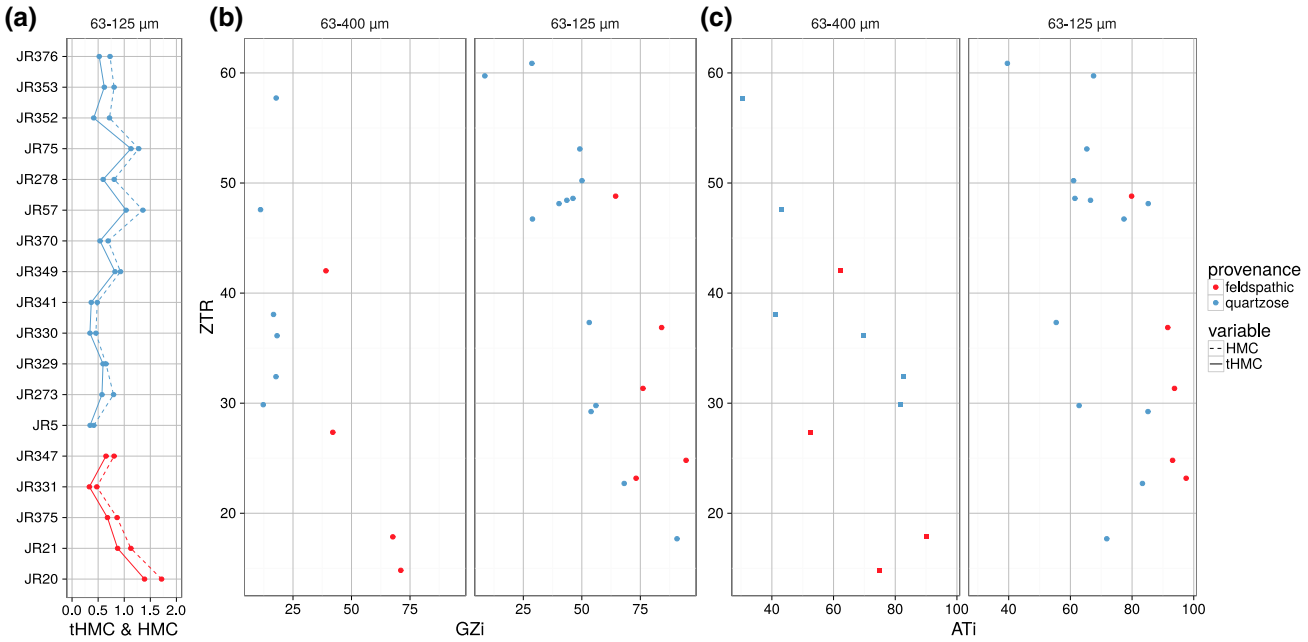

Fig. 12 Heavy-mineral indices. **a** tHMC: transparent heavy-mineral content (Garzanti and Andò 2007), **b** ZTR versus GZi (garnet/garnet + zircon) and **c** ZTR versus ATi (apatite/apatite + tourmaline) from Morton and Hallsworth (1994)

Dickinson model (Fig. 9). This may occur in a fluvial system by the migration of the river bed (Amorosi and Zuffa 2011) or in marine basins through the influence of an oceanic current (Morton and Hallsworth 1999). Likewise, the scattered presence of metamorphic fragments (Fig. 11h, i) could also result from the reworking of deposits related to the Feldspathic petrofacies. Following the Garzanti model (Garzanti et al. 2007), the Quartzose petrofacies provenance can correspond either to the continental block or to the clastic wedge provenance.

Intrabasinal components, including chemical (glauconite and phosphate) and biological (bioclasts and micritic limestones) grains, are frequent in the samples from the Quartzose petrofacies. They indicate the reworking of platform sediments by gravity currents, especially during transgressive phases (Odin and Matter 1981; Garzanti 1991). A high amount of carbonate grains is characteristic of close-up basins (Critelli et al. 2007), and controls diagenetic processes such as cementation and porosity reduction (Fig. 18). The reworking of sediments could also be explained by the influence of marine currents (Ingersoll 1990, 1993) especially during sea-level highstands (Amorosi and Zuffa 2011). Hence, both allogenic and autogenic

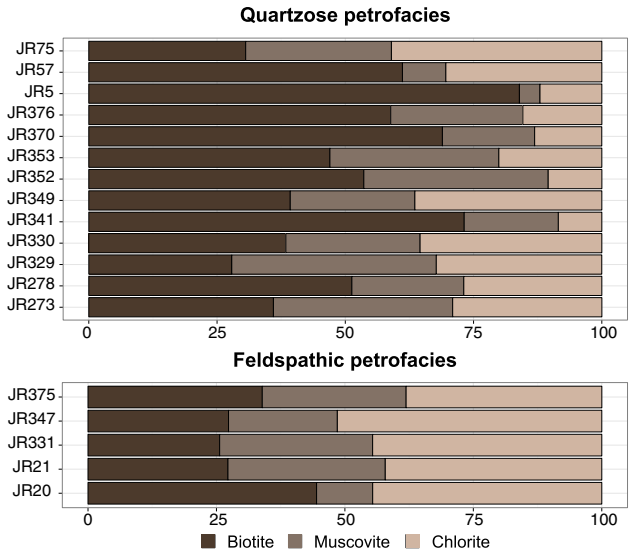

Fig. 13 Mica distribution in the 63–125 µm fraction

factors controlled the composition of the Quartzose petrofacies.

Provenance of the Feldspathic petrofacies

The feldspar-dominated (Fig. 9) assemblage indicates a location in the basement uplift to dissected volcanic arc fields of the Dickinson model (Dickinson 1985; Dickinson and Suczek 1979). However, the source rocks are quite similar to those of the Quartzose petrofacies (Figs. 11, 14). The main difference lies in the low sediment maturity in the Feldspathic petrofacies. Hence, it presents a lithic-rich composition (Figs. 9, 11) with some andesitic and granitic rock fragments. The main characteristic of the Feldspathic petrofacies is the abundance of metamorphic lithics and rock fragments in sand-size grains (Fig. 11), and especially of the psammite-derived metamorphic lithics according to the colour guide of Garzanti and Vezzoli (2003). Polycrystalline quartz (QpT) is a good indicator of these metamorphic inputs (Fig. 11d). The occurrence of staurolite (amphibolite facies), rutile (HP grade) (Fig. 14) and chlorite (low-grade metamorphism) (Fig. 15) suggest a large variability of metamorphic rocks. They are presumably related to regional metamorphism and to low- to intermediate-grade meta-sediments (von Eynatten and Gaupp 1999; Copjakovà et al. 2005; von Eynatten and Dunkl 2012). The association of garnet and staurolite may indicate a source in micaschist complexes (Füchtbauer 1964). According to the Mange and Morton (2007) garnet discrimination diagram (field Bi, Fig. 15b), the almandine-dominated garnet distribution (Alm and Alm-Prp) mostly corresponds to amphibolite-grade (MP-MT) metasedimentary rocks, thus corroborating the high metamorphic grade (Fig. 9e, f). The small amount of Alm-Sps and Sps-Alm-Grs could derive from granites and pegmatites or from metamorphic rocks such as higher greenschist facies. (Krippner et al. 2014, field B Fig. 15b), whereas the scarce Grs may originate from contact metamorphosed marls or calcareous shale (Win et al. 2007). Besides, the low amount of pyrope precludes peridotite and eclogite source rocks (von Eynatten and Gaupp 1999).

The high amount of metamorphic grains correlates the Feldspathic petrofacies with the Axial belt provenance (Garzanti et al. 2004, 2007, 2010). Such a provenance favours the entrainment of fresh material in the sedimentary cycle. However, the similarity with the Quartzose petrofacies strongly suggests that sediments of both petrofacies

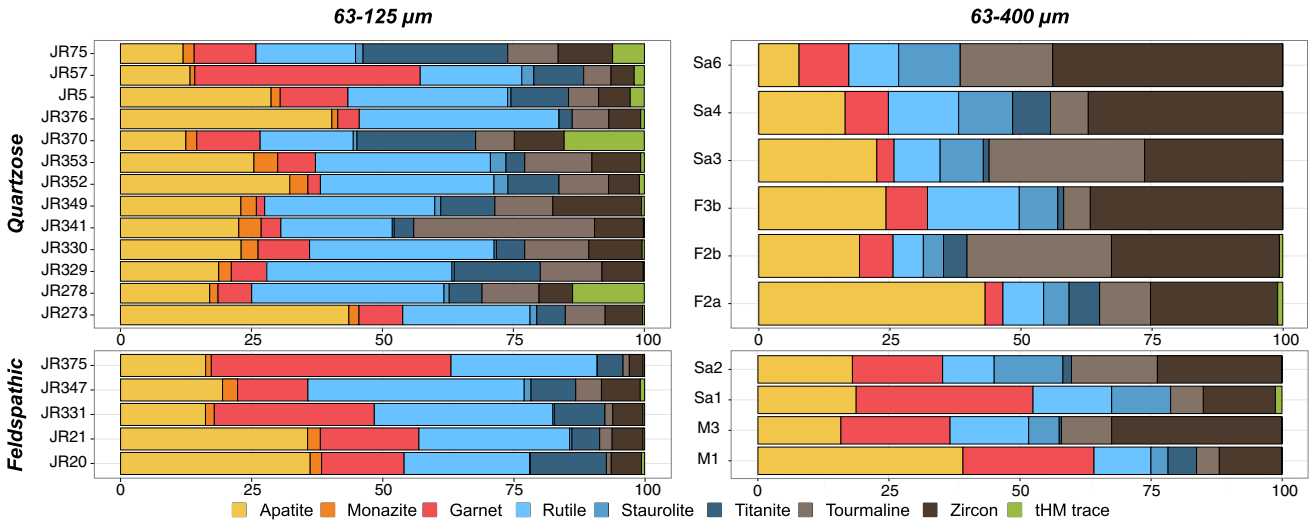

Fig. 14 Transparent heavy-mineral distribution for the 63–125 µm and recounted 63–400 µm fractions

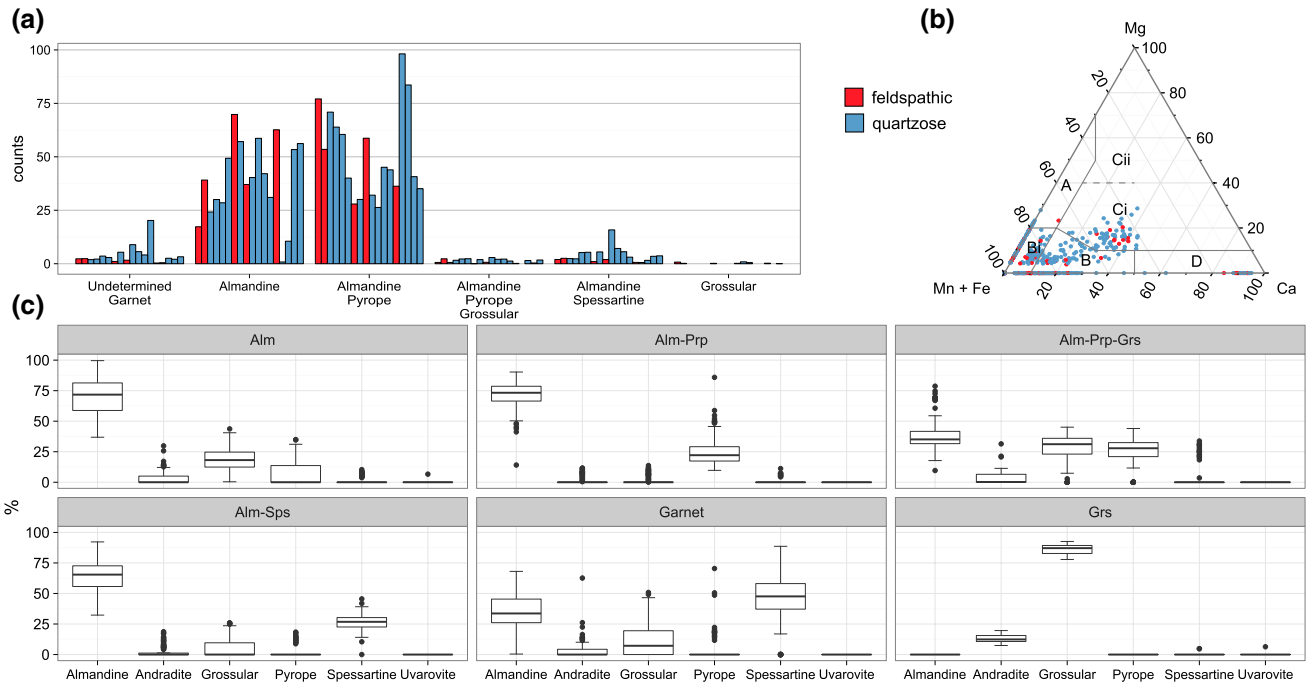

Fig. 15 Garnet geochemistry. **a** Relative distribution of the different classes identified by the QEMSCAN®, **b** ternary diagram of garnet discrimination after Mange and Morton (2007), **c** SEM-EDS composition of the different garnet classes based on end-member abundances. For key to box plots see Fig. 8

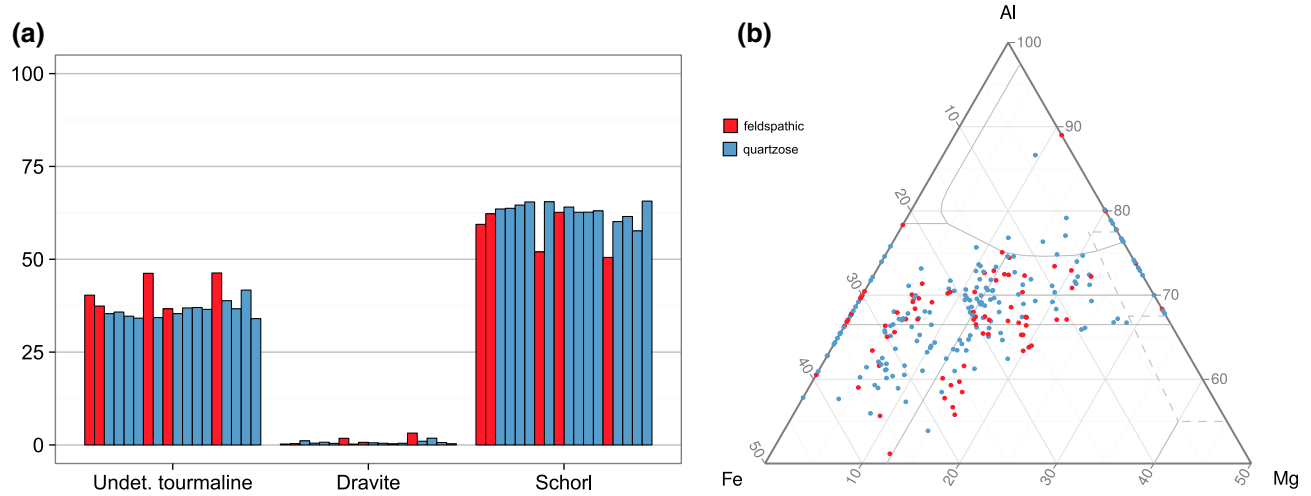

Fig. 16 Tourmaline geochemistry, **a** relative distribution of the different classes identified by the QEMSCAN®, **b** ternary diagram of tourmaline discrimination after Henry and Guidotti (1985)

met comparable weathering conditions, regarding the scarcity of the other typical metamorphic unstable grains.

Intrabasinal grains (NCI and CI grains) are scarce in the Feldspathic petrofacies (Fig. 18) suggesting a reduced marine influence in the sand composition and a sparse cementation linked to the low carbonate content. Hence, allogenic factors, especially tectonics, controlled sediment composition of the Feldspathic petrofacies. This may explain the formation of this relatively unaltered proximal facies which is usually associated to sea-level lowstands (Amorosi and Zuffa 2011).

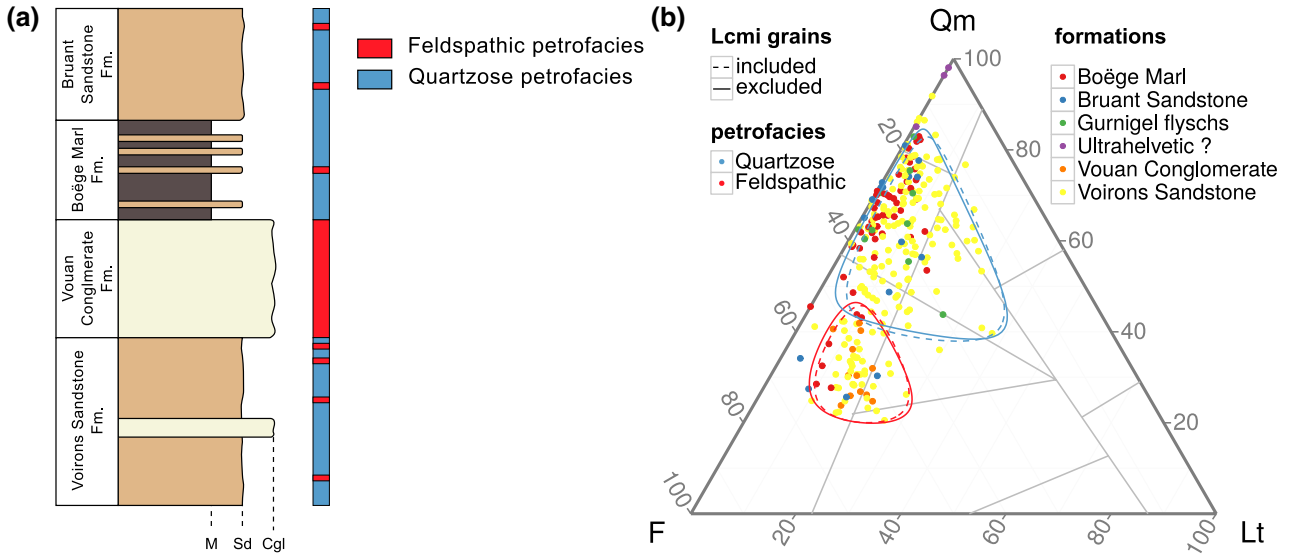

Fig. 17 Relationship between petrofacies and stratigraphic units illustrated by a synthetic log of the Voirons Flysch (**a**) and the QmFLt ternary diagram (Fig. 8b) with the initial stratigraphic affiliation (**b**). Note the widespread location of most of the stratigraphic units

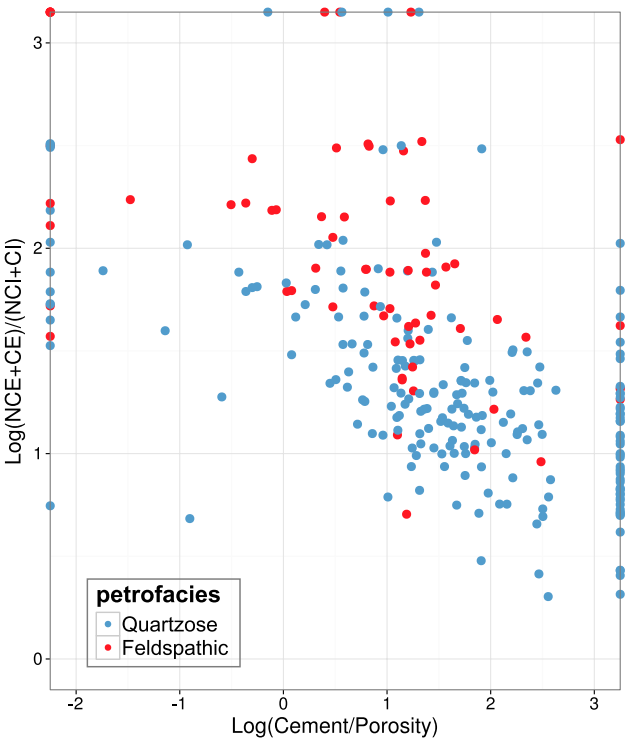

Fig. 18 Relationship between extrabasinal vs. intrabasinal grains and cement vs. porosity

Regional comparison with the other Prealps flyschs

Our data are compared with the following flysch deposits exposed in the Prealps (Figs. 1, 2, 3): (1) the Upper Prealps flyschs (Caron 1972; Flück 1973; Gasinski et al. 1997) represented by the Sarine, the Dranses and the Simme flyschs—South Penninic domain, (2) the Médianes Flysch (Flück 1973; Caron et al. 1989)—Briançonnais domain, (3) the other flyschs from the Gurnigel nappe represented by the Schlieren (Winkler 1983, 1984) and the Wägital flyschs (Winkler et al. 1985b) and (4) the Niesen flyschs (Ackermann 1984, 1986)—Valais domain. The petrography of these units has been studied during the 1970–1980's following the Gazzi-Dickinson method (Fig. 19), and salient results are compiled in Caron et al. (1989).

The first phase of flysch deposition in the Alps is represented by the Simme and the Gets flyschs. They are devoid of garnet grains, but contain a variable amount of chrome-spinel (Fig. 20a) which is inherited from the Piemont ophiolites (Bertrand and Delaloye 1976; Bill et al. 1997; Beltran-Trivino et al. 2013). Their lithic-rich composition (Fig. 19a) emphasises massive inputs of fresh material from both continental and oceanic crusts (Gasinski et al. 1997 and references therein). Framework composition describes a recycled orogen tectonic setting (Dickinson and Suczek 1979) and an Ophiolite provenance (Garzanti et al. 2007), considering the spinel-rich heavy-minerals. They do not share any petrographic similarities with the flyschs from the Gurnigel nappe (Fig. 19a).

The younger Sarine and Dranses flyschs have a similar framework composition characterised by a low lithic content (Fig. 19a). However, the heavy-mineral populations are very different from the Simme and the Gets flyschs (Fig. 20a). The low garnet content indicates minor metamorphic inputs, whereas the high proportion of zircon and tourmaline indicates a granitic source. These flyschs plot in the continental block to clastic wedge provenance

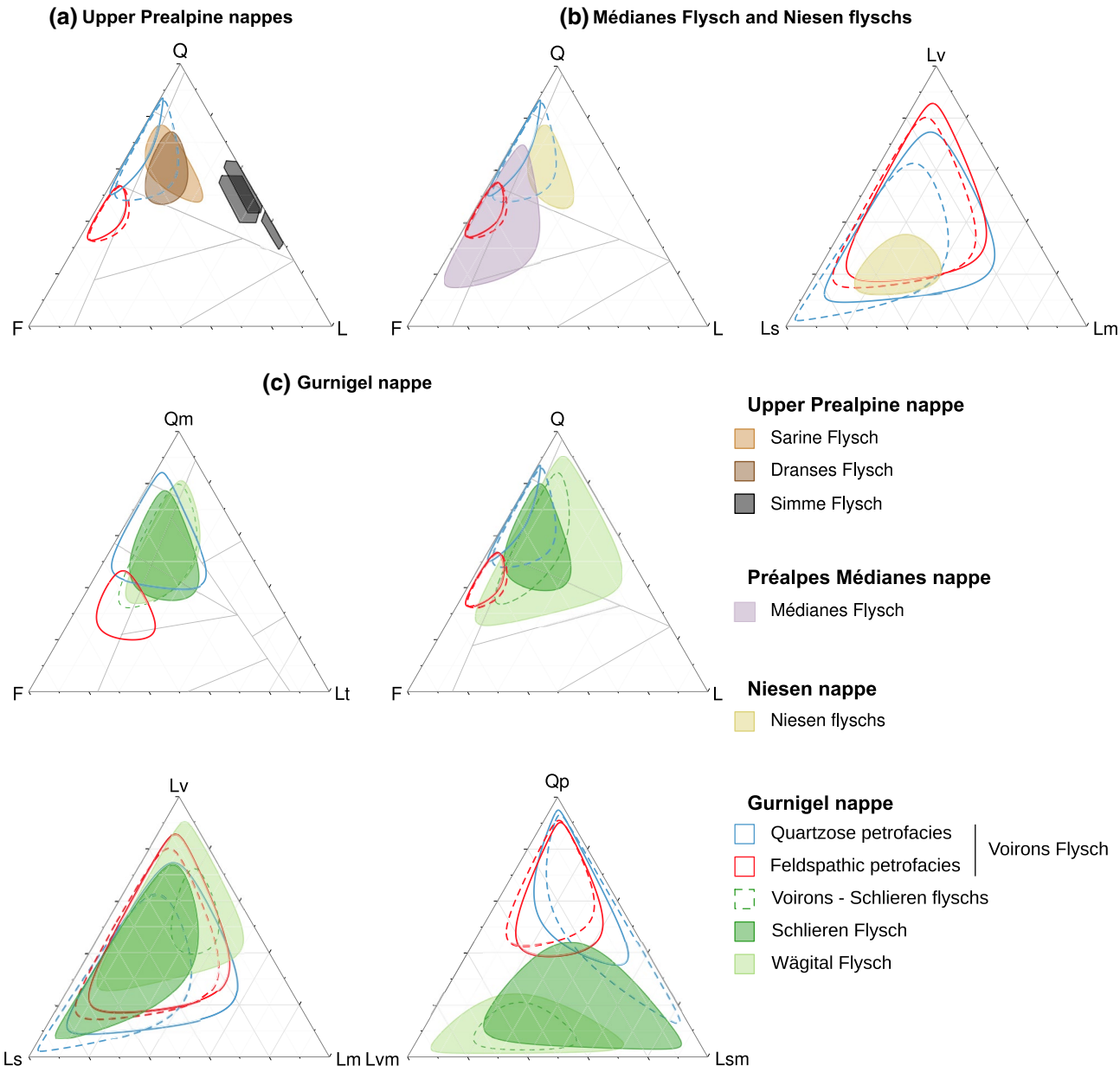

Fig. 19 Ternary diagrams of the Dickison model of the Voirons Flysch provenances compared to the Upper Prealps flyschs (**a**), the Médianes Flysch and the Niesen flyschs (**b**) and the other Gurnigel flyschs (**c**). See references in text

according to the Garzanti model (Garzanti et al. 2007). Their location in the transitional continental to mixed tectonic settings (Dickinson and Suczek 1979; Dickinson 1985), as well as the low garnet content, is similar to that of the Quartzose petrofacies (Fig. 19a).

The composition of the Médianes Flysch is characterised by a feldspar-dominated composition. Garnet grains occur in the heavy-mineral assemblage of this flysch, but seems to be missing in the Brèche Flysch (Fig. 15). The rare chrome-spinel grains found in the Médianes Flysch (Flück 1973) are likely reworked from the Simme or the Gets flyschs (Beltran-Trivino et al. 2013). Provenance interpretation defines a basement uplift tectonic setting (Dickinson and Suczek 1979; Dickinson 1985). The composition of the Médianes Flysch is very similar to the Feldspathic petrofacies of the Voirons Flysch, but is richer in lithic fragments (Fig. 14b). Scarce data from the Brèche Flysch preclude any provenance interpretation.

The Schlieren and Wägital flyschs plot in the transitional continental to mixed fields of the Dickinson model. These units appear to differ from the Quartzose petrofacies because of the different interpretation of micritic lithoclasts

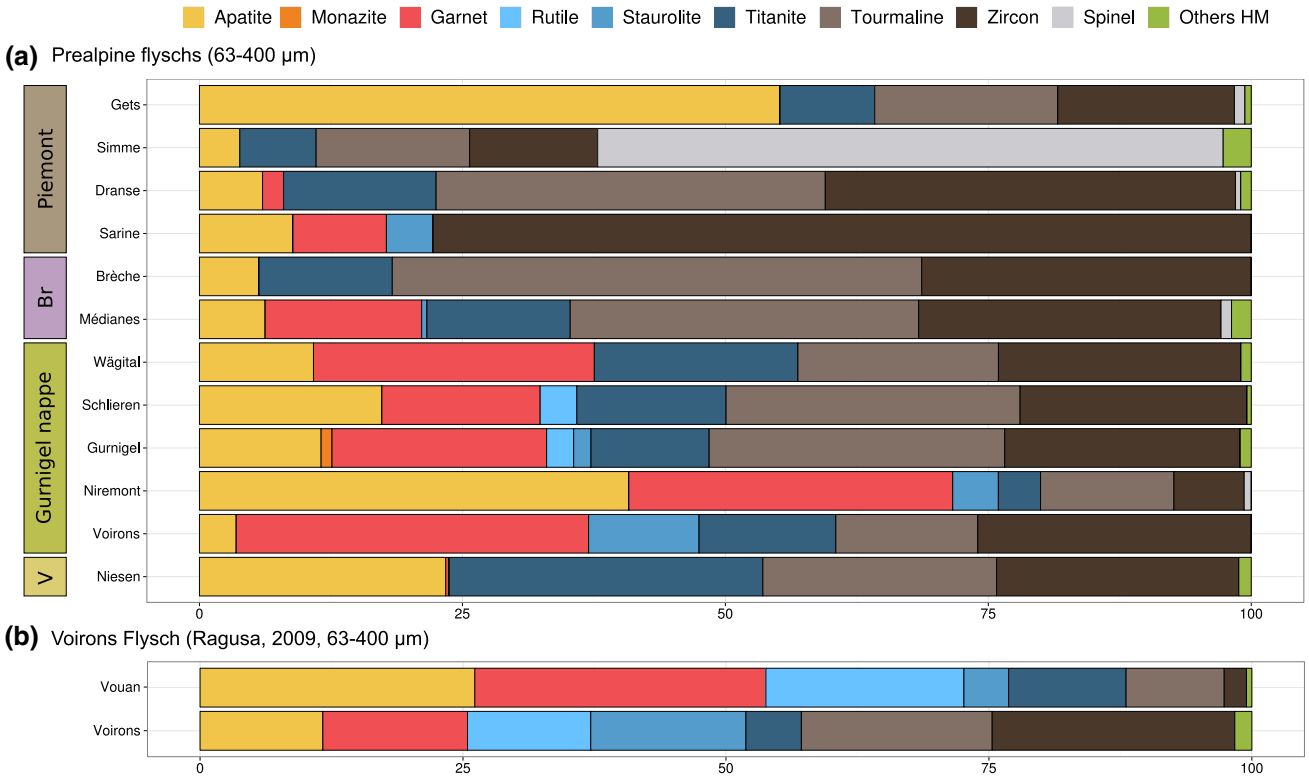

Fig. 20 Transparent heavy-mineral distribution in the Prealps flyschs (**a**) and mean distribution from the Voirons. Flysch with 63–125 and 63–400 µm range (Ragusa 2009, modified) (**b**). *Br* Briançonnais domain, *V* Valais domain. See references in text

and by a richer content in polycrystalline quartz. Incorporation of the micritic grains (Fig. 15c; dashed lines) in the counting provides similar results. The Wägital Flysch is characterised by an elevated content in metamorphic and volcanic lithoclasts. Garnet and staurolite contents are high and equivalent to the zircon + tourmaline content. The Schlieren Flysch is rich in sedimentary lithoclasts, with the notable presence of dolostone fragments likely derived from Triassic deposits (Winkler 1983, 1984). Metamorphic inputs decrease, and the granitic source rather influences the heavy-mineral assemblage. Based on the ATi values (Bütler et al. 2011), two different magmatic provenances are reported for the Schlieren Flysch: a granitic–rhyolitic source and a tonalitic–andesitic source. The Niremont Flysch shows a particularly elevated content in apatite and garnet associated with a low content in ultrastable minerals (Fig. 20). No framework composition is available for this flysch.

The overall composition of the flyschs from the Gurnigel nappe shares many similarities, and confirms the uniqueness of this nappe (Fig. 19c). The heavy-mineral population consists of a garnet + ZTR-dominated assemblage and a variable amount of apatite in all these flysch deposits (Fig. 20; Wildi 1985). However, differences in the lithoclast distribution (Fig. 14c) suggest a compositional variation from East to West (Winkler 1984), which may indicate a lesser unroofed basement source in the West. However, this does not appear in the heavy-mineral distribution. Hence, the composition evolves from a magmatic and metamorphic source in the East to a more sedimentary-rich supply in the Voirons Flysch (Fig. 19c, QpLvmLsm diagram), showing that the crystalline sources are progressively diluted by a greater amount of sedimentary detritus.

The similar framework composition and heavy-mineral assemblage confirm the affinity of the Quartzose petrofacies from the Voirons with the rest of the Gurnigel nappe (Fig. 19c). The occurrence of samples from the Fayaux and Zollhaus quarries in this branch confirms the similarity of this source with the detrital sources reported for the other flyschs of the Gurnigel nappe (Winkler 1983, 1984; Caron et al. 1989), which is also corroborated by the presence of pink granite fragments (Fig. 6a). However, based on the ATi values (Fig. 12), the granitic–rhyolitic source of the Schlieren Flysch (Bütler et al. 2011) is not present in the Voirons Flysch. The large distribution of the Wägital Flysch slightly overlaps the Feldspathic petrofacies, and the content in metamorphic lithics shows some affinity which cannot be further resolved. However, the massive Vouan Conglomerate Fm. is not reported from any other flysch

deposits in the Gurnigel nappe (Caron et al. 1989). The lack of pink granite pebbles in this formation further demonstrates the quasi-uniqueness of the Feldspathic petrofacies in the Voirons Flysch.

The zircon geochronology (Beltran-Trivino et al. 2013) and the lack of garnet (Wildi 1985; Bernoulli and Winkler 1990; Argnani et al. 2004) indicate a detrital source located along the northern Tethyan margin for the Niesen flyschs (Wildi 1985). Despite the distinctive detrital provenances, no significant differences in in the QFL ternary diagram have been observed between these flyschs and those from the Gurnigel nappe (Fig. 19b). These similarities are linked to the homogeneous composition of rock sources along the northern margin of the Alpine Tethys characterised by granitic rocks and sedimentary covers shared with the Ultrahelvetic realm (Ackermann 1986; Lihou and Mange-Rajetzky 1996).

This review emphasises the similar framework composition and heavy-mineral assemblage of several Prealps flyschs derived from the southern Tethyan margin: the Dranses Flysch, the Sarine Flysch, the Médianes Flysch and the flyschs from the Gurnigel nappe. Such resemblances result not only from similar rock sources, but also from the cannibalisation of these flyschs that were progressively incorporated into the sedimentary accretionary prism, and fed the subsequent flysch deposits. They also suggest a gradual tectonic evolution of the accretionary wedge and the surrounding crystalline basement (Fig. 21). Sedimentary inputs were initially dominated by stable-rich grains (e.g. ZTR province of Wildi 1985) originating from plutonic crystalline basement and sedimentary covers. Punctual reworking of oceanic crust (e.g. Cr-Spinel province of Wildi 1985) indicates that residual ophiolite were exposed in front of the southern Tethyan margin (Gasinski et al. 1997). They were progressively replaced and/or associated with metamorphic rock source related to the uplift of the metamorphic belt (e.g. Garnet province of Wildi 1985). The transition ZTR to Garnet province should be related to the closure of the Piemont Ocean and the subduction of the Briançonnais microcontinent.

Considering the framework composition and heavy-mineral assemblage, the Quartzose petrofacies could have been fed by the Dranses and/or the Sarine flyschs, whereas the Feldspathic petrofacies could originate from the Médianes Flysch. Finally, the different composition within the Gurnigel nappe emphasises different sedimentary systems inherited from the tectonic deformation of the sedimentary accretionary prism.

Geotectonic model of the Voirons Flysch

The petrographic and mineralogical data presented in this study show that, like the other flyschs of the Gurnigel nappe, the constituent material of the Voirons Flysch originates from the southern margin of the Alpine Tethys (Bütler et al. 2011). Five major age populations were identified in the detrital zircons (610–550, 510–490, 468–425, 346–315, 205 Ma; Fig. 23; Bütler et al. 2011) corresponding to the different palaeogeographic province of the Tethyan realm. The paleocurrent pattern of the Gurnigel nappe indicates a northern direction which is deflected eastward along the oceanic trench (Caron et al. 1980; Winkler 1984; Wildi 1985) (Fig. 24). Both the paleocurrent pattern and biostratigraphy further suggest a westward migration of the detrital source linked to the scissor closure of the basin (Winkler 1984). Moreover, biostratigraphic work by Ujetz

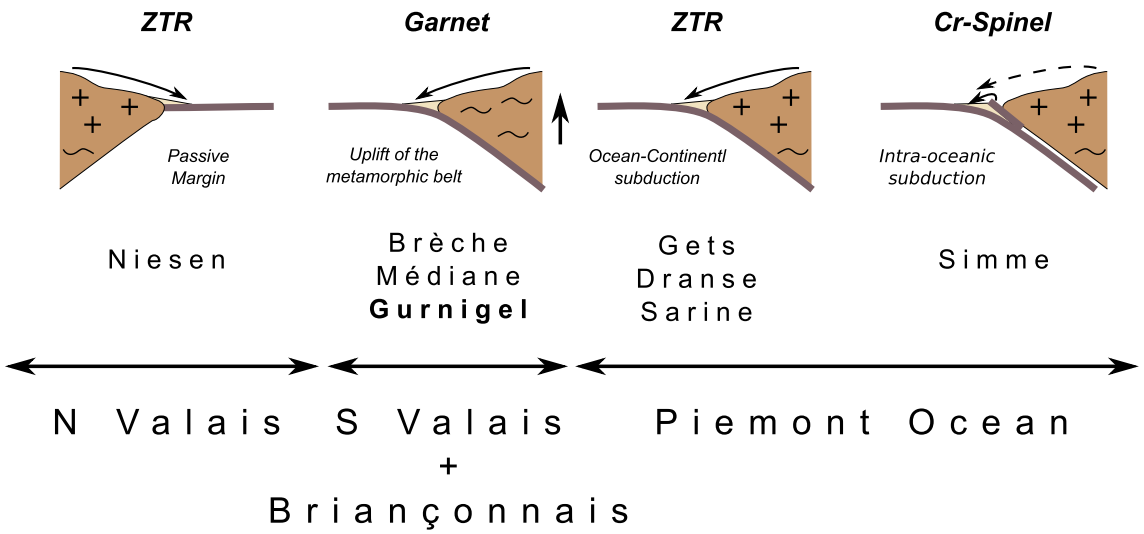

Fig. 21 Synthetic model of the evolution of tectonic settings during the Tethyan close-up and the respective heavy-mineral provinces of Wildi (1985)

(1996) and, more recently, Ospina-Ostios et al. (2013) showed that the sedimentation of this flysch took place in a time interval between the Middle Eocene and the Late Eocene/Early Oligocene. In this period, the sedimentary accretionary prism comprised the Briançonnais and Piemont sedimentary covers (Mosar et al. 1996, Fig. 7) and, in the highest position, of the Sesia–Dent Blanche nappe (Schmid et al. 1996; Handy et al. 2010) (Fig. 25). The latter of which was partially obducted and formed the back stop of the Alpine Tethys accretionary prism (Stampfli et al. 1998; Manzotti et al. 2014). This prism was separated from the Southern Alps by the Periadriatic fault. Hence, no sediments from the Southern Alps could contribute to flysch deposition in the Alpine Tethys, except for those already reworked during the initiation of subduction (e.g. the Simme Flysch) explaining how Southern Alps-derived volcanic grains of Triassic age (205 Ma peak, Fig. 23) occur in the Gurnigel nappe (Bütler et al. 2011) and Médianes Flysch (Beltran-Trivino et al. 2013). In addition, the detrital zircon population pertaining to 468–425 Ma peak can also be related to the Southern Alps.

The Sesia–Dent Blanche nappe is composed of an igneous basement and of sedimentary covers metamorphosed during the Late Cretaceous (Manzotti et al. 2014). It formed the metamorphic belt of the Tethyan accretionary prism (Figs. 23, 24). The geochemistry of garnets from the Voirons Flysch suggests derivation from metasedimentary rocks and (metamorphosed?) igneous rocks of similar composition to those described from the Sesia–Dent Blanche nappe (Fig. 22). Alm-Prp-Grs and Grs-And grains are indeed reported in metapelite; metabasite and calcsilicate rocks respectively from this unit (Dal Piaz et al. 1983). The former may also derive from recycled kinzigite preserved in the Eclogitic Micaschists Complex. A potential

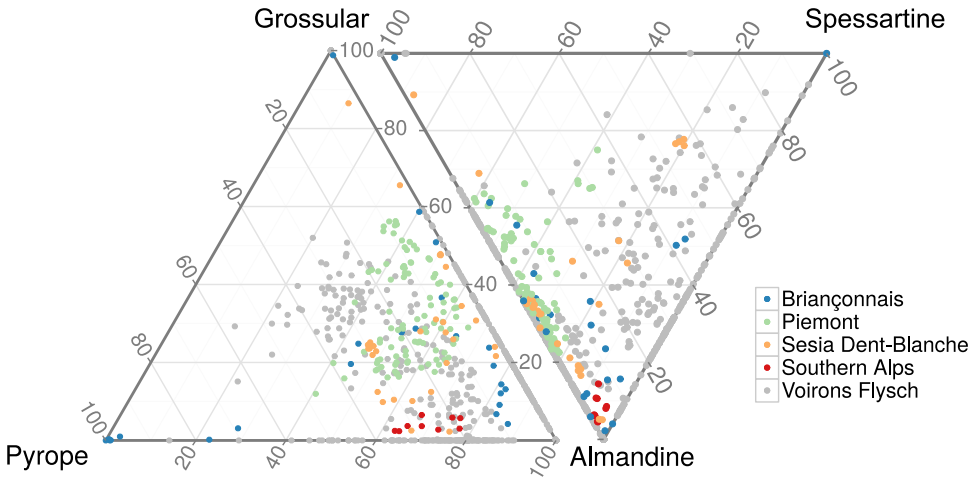

Fig. 22 Major garnet end-member ternary diagram of middle to upper Penninic domains based on compilation of Stutenbecker et al. (2016). Briançonnais: Thélin et al. (1990), Schertl et al. (1991), Giorgis et al. (1999), Bucher and Bousquet (2007); Piemont: Oberhänsli (1980), Cartwright and Barnicoat (2002), Bucher and Grapes (2009), Weber and Bucher (2015); Sesia–Dent Blanche: Dal Piaz et al. (1983), Gardien et al. (1994), Kirst (2014); Southern Alps: Hunziker and Zingg (1980)

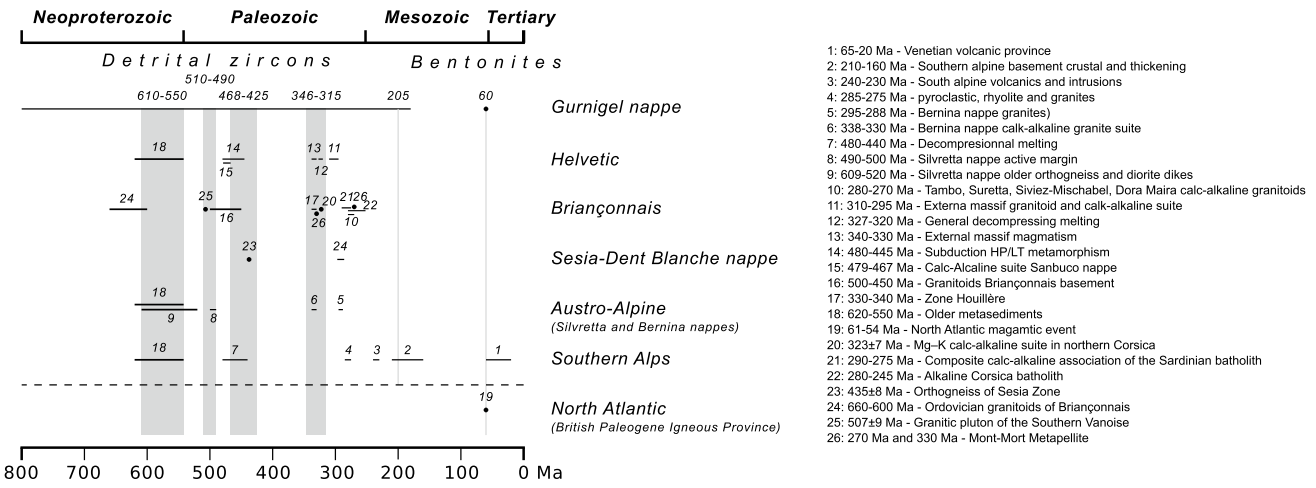

Fig. 23 Major U/Pb age peaks of the detrital zircons (Bütler et al. 2011) and bentonites (Koch et al. 2015). Data are compared to the major magmatic events in the Tethyan realm based on the modified compilation of Bütler et al. (2011). Bütler et al. (2011): *1–16*; Schaltegger and Gebauer (1999): *18–24,25*; Koch et al. (2015): *19*; Cortesogno et al. (1998): *20–22*; Manzotti et al. (2014): *23*; Bussy et al. (1996): *26*

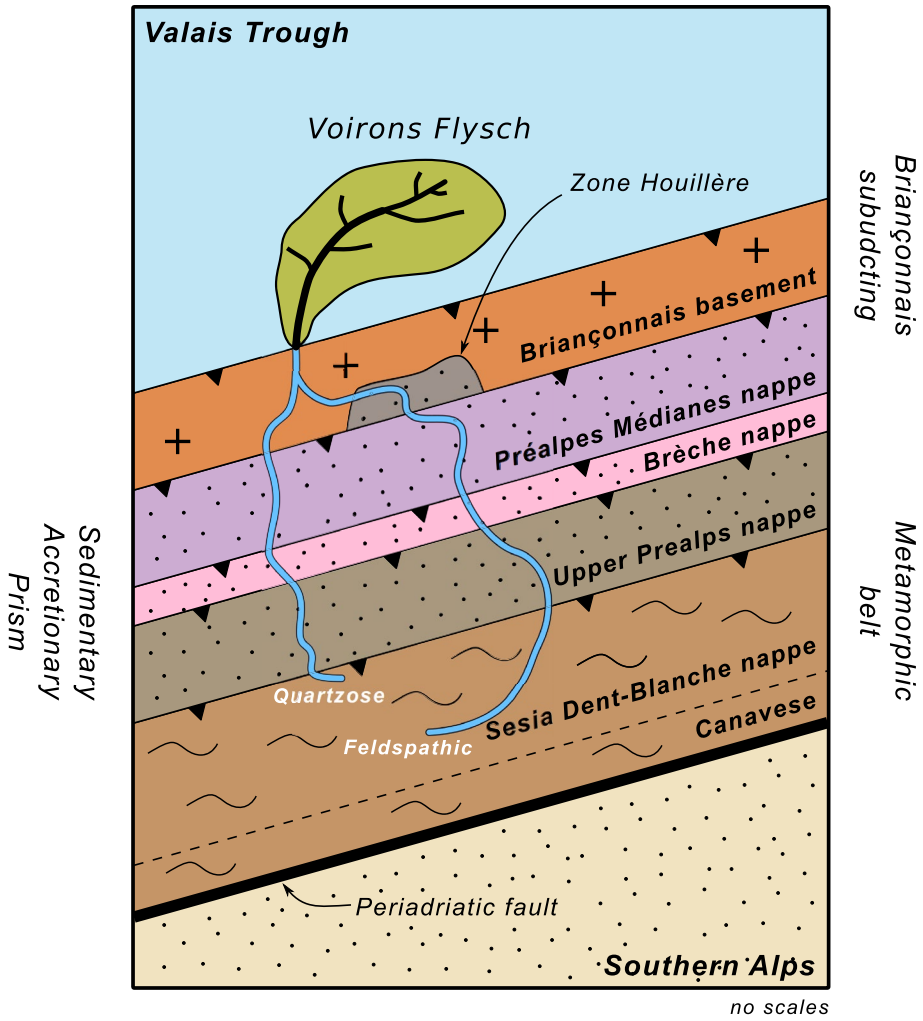

Fig. 24 Paleogeographic model of the Voirons Flysch and its two different detrital sources

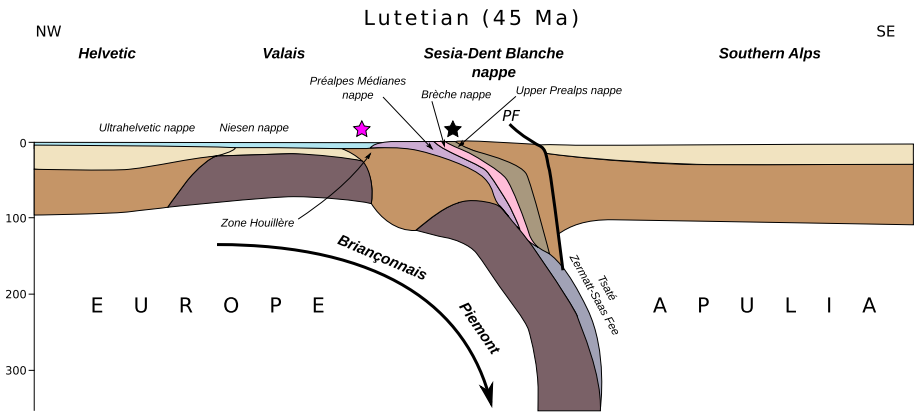

Fig. 25 Cross section of the Tethyan realm during the Lutetian (Handy et al. 2010, modified). The *stars* indicates the paleogeographic location of the Voirons Flysch considering a Paleocene to Middle Eocene (*black*) and Middle to Late Eocene age (*purple*)

clinopyroxene-rich amphibolite from the Valpelline serie is also envisaged considering the metabasite source. Our data are in agreement with the garnet geochemical data of Kirst (2014) from metasedimentary rocks of the Becca d'Aver continental sliver. Almandine-rich garnet is also reported in the Lombardian Flysch of the Southern Alps (Bernoulli and Winkler 1990) corroborating that the Sesia–Dent Blanche nappe could be the source of garnets. Despite tourmaline being widespread in the Alps, geochemical data are scarce, preventing constraints on their origin. Finally, the few geochronological data (Manzotti et al. 2014 and Fig. 23) obtained from the Sesia–Dent Blanche nappe could correspond to the 468–425 Ma range reported by Bütler et al. (2011).

Rare andesite lithoclasts observed in the Voirons Sandstone Fm. (Ospina-Ostios et al. 2013, Fig. 4) cannot originate from the Sesia–Dent Blanche nappe due to the Oligocene age of the andesite layers from the external part of the Sesia-Lanzo unit (Venturelli et al. 1984, and references therein). Nevertheless, Upper Carboniferous–Permian volcanic deposits relating to the Variscan orogeny (Cortesogno et al. 1998) are a potential source of andesite grains. Volcanic Upper Carboniferous–Permian units are reported from (1) the Ligurian Alps and Sardinia in the Briançonnais domain (Cortesogno et al. 1998; Decarlis et al. 2013) and the Siviez-Mischabel nappe (Sartori et al. 2006), and (2) the Southern Alps (Cortesogno et al. 1998) through the Simme nappe. Most of this event may have been poorly preserved in detrital zircon or poorly contribute to the detrital sedimentation. Hence, the 310–260 Ma interval constitutes secondary peak and rarely high-frequency peak (Bütler et al. 2011; see sample 11EB07 in 280–300 Ma range for the latter). However, the oldest component may represent or at least contribute to the 346–315 Ma population of the detrital zircon (Bütler et al. 2011; Fig. 23). A derivation from a volcanic arc developed along the southern Tethyan margin during the subduction of the Piemont Ocean (Gasinski et al. 1997) is excluded on the basis of a lack of coeval ages in detrital zircon (Bütler et al. 2011; Beltran-Trivino et al. 2013), and bentonite layers (Winkler et al. 1985a, 1990) might derive from the British Paleogene Igneous Province (Koch et al. 2015).

Likewise, the black sandstones pebbles of Paleozoic age (Fig. 6b) reported from the Vouan Conglomerate Fm. likely indicate an input from the Briançonnais basement. Such pebbles possibly originate from the Palaeozoic rift basin of the Zone Houillère (Fabre 1961). In addition, recent detrital zircon geochronological data from the Dora Maira massif and the Zone Houillère (Manzotti et al. 2016) constrain the magmatic events between 330 and 340 Ma which correspond to the 346–315 Ma peak (Fig. 23). Moreover, a similar almandine-rich garnet geochemistry is reported from the Briançonnais basement (Fig. 22). An Alm-Prp-Grs composition is reported from the Siviez-Mischabel nappe (Thélin et al. 1990) as well as Alm-Sps composition from the Zone Houillère (Bucher and Bousquet 2007) and Pontis nappe (Giorgis et al. 1999). However, pyrope grains documented in the Dora Maira massif by Schertl et al. (1991) are absent. The combination of data suggests that the Briançonnais basement during its subduction is a likely detrital source (Fig. 24). Nevertheless, distinguishing this detrital source from the Sesia–Dent Blanche nappe remains problematic and might be resolved using additional analysis such as garnet geochronology (Baxter and Scherer 2013).

Finally, the older detrital zircon geochronological data are widespread distributed and hence cannot constrain the detrital source. The 510–490 Ma range (Fig. 23) is reported from the Briançonnais domain and the Austro-alpine Silvretta nappe (Schaltegger and Gebauer 1999). The 610–550 Ma range (Fig. 23) is linked to the oldest metasediments in the Briançonnais, Austro-alpine and Southern Alps (Schaltegger and Gebauer 1999). In addition, although they match with several peaks (610–550, 468–425 and 346–315 Ma, Fig. 23), zircon ages from the northern Tethyan margin are irrelevant since no southward paleocurrent is described in the Gurnigel nappe.

The exhumed metamorphic lithologies of the Sesia–Dent Blanche nappe, and to a lesser extent of the Briançonnais basement, could likely represent the basement uplift tectonic setting (Dickinson et al. 1985) or the axial belt provenance (Garzanti et al. 2004, 2007, 2010) of the Feldspathic petrofacies (Fig. 9). This is in agreement with the feldspar-dominated and garnet-rich detrital composition of modern fluvial sediments shed by the Dent Blanche nappe (Garzanti et al. 2010). The accretionary prism fed the flysch deposits with reworked detrital grains of various lithologies (calcareous to crystalline rocks) (Fig. 24). These reworked sediments were depleted in unstable grains which gave them a mature composition (Velbel 1985). The resulting detrital composition reflects the clastic wedge provenance of the Garzanti model (Garzanti et al. 2007) and the transitional continental to mixed tectonic setting (Dickinson et al. 1985) of the Quartzose petrofacies (Fig. 9).

This palaeogeographic model of the Voirons Flysch (Fig. 24) differs from the well-accepted model applied to the other flyschs from the Gurnigel nappe (Winkler 1983, 1984; Caron et al. 1989). The latter considers a Maastrichtian to Lutetian age (Van Stuijvenberg 1979; Van Stuijvenberg and Jan du Chêne 1980; Winkler 1983, 1984), and constrains the deposition of the Gurnigel flyschs in a Piemont Ocean characterised by a sedimentary accretionary prism that was smaller at that time than in the Middle Eocene to Late Eocene/Early Oligocene (Fig. 25). Based on the palaeogeographic reconstructions for the Early Cenozoic (Schmid et al. 1996; Handy et al. 2010), the suggested detrital sources for these flyschs are restricted to the Sesia–Dent Blanche nappe and the Upper Prealps nappes (Fig. 25). The dispute thus lies on the younger age obtained for the Voirons Flysch (Ujetz 1996; Ospina-Ostios et al. 2013), which precludes deposition in the Piemont domain. Further biostratigraphic investigations are needed to clarify the palaeogeographic locations for the entire Gurnigel nappe. As long as the biostratigraphy of this nappe is not completely resolved, the relationship of the Voirons Flysch with the rest of the Gurnigel nappe, and their respective palaeogeographic locations, remain a matter of debate.

Temporal evolution of the detrital inputs

The correlation of the petrofacies of the Voirons Flysch with the stratigraphy shows a temporal variation in the sediment supplies (Fig. 17a) as already suggested by Winkler (1984) for the rest of the Gurnigel nappe. Deposition began during the Middle Eocene with the Quartzose petrofacies in the Voirons Sandstone Fm. The source of the Feldspathic petrofacies was barely active at that time. In Late Eocene, inputs from the Feldspathic petrofacies markedly increased and alternated with those from the Quartzose petrofacies which progressively decreased. The fading of the Quartzose petrofacies concurred with the progradation of the turbiditic system and the deposition of the Vouan Conglomerate Fm. During these events, the source of the Quartzose petrofacies was either inactive or the detritus was shed to a different basin which remains unknown. The sharp contact between the Vouan Conglomerate Fm. and the Boëge Marl Fm. marks an abrupt modification both in the turbiditic system (development of a starved system) and in the sediment supply (the Quartzose petrofacies returns as the dominant supply) which may be related to major tectonic events. Finally, the gradual evolution towards the Bruant Sandstone Fm. indicates a steady-state system with an increase of sand-shale ratio dominated by the Quartzose petrofacies and sporadic inputs of the Feldspathic petrofacies.

Conclusions

Our study of the Voirons Flysch complements the existing dataset on the petrography of the flyschs from the Gurnigel nappe, and offers a new interpretation of the provenance of its constituent material.

1. In contrast to the other flysch units from the Gurnigel nappe, two distinctive sources have been identified in the Voirons Flysch,

- The Quartzose petrofacies is the major detrital source. It is similar to the provenances described elsewhere in the Gurnigel nappe. It is a quartz-rich assemblage with sedimentary to magmatic lithoclasts and a heavy-mineral assemblage dominated by ZTR + apatite. The most salient clasts in the conglomerate layers are pink granite fragments. The lithic composition variation reflects polycyclic sedimentary inputs corresponding to a transitional continental block tectonic setting (Dickinson and Suczek 1979) or a Clastic wedge provenance (Garzanti et al. 2007).
- The Feldspathic petrofacies represents a subordinate source in the Voirons Flysch, and has up to now not been identified elsewhere in the Gurnigel nappe. The Feldspathic petrofacies is mostly restricted to the Vouan Conglomerate Fm. Rock-fragment composition is characterised by black sandstones of Paleozoic age in conglomeratic layers. Garnet dominates the heavy-mineral assemblage, and metamorphic lithoclasts describe an axial belt provenance (Garzanti et al. 2007) or a basement uplift tectonic setting (Dickinson and Suczek 1979) considering the feldspar-rich composition. Samples distribution shows punctual inputs of this secondary detrital source during deposition of the Quartzose petrofacies.

2. The random deposition of the Feldspathic petrofacies within lithologic units dominated by the Quartzose petrofacies, as well as the interfingering contact between the Voirons Sandstone Fm. and the Vouan Conglomerate Fm. confirm the stratigraphic nature of the contacts within the Voirons Flysch.
3. A comparison of the Voirons Flysch with the Sarine and Dranses flyschs shows a similar quartz-rich composition, which indicates a similar source along the southern Tethyan margin and/or reworking of the latter deposits in the former.
4. A palaeogeographic location of the Voirons Flysch in the Valais domain is suggested considering (1) the Middle Eocene to Late Eocene/Early Oligocene age obtained from planktonic foraminifera biostratigraphy (Ujetz 1996; Ospina-Ostios et al. 2013), (2) the marked similarity of the black sandstone lithoclasts of Paleozoic age found in the Vouan Conglomerate Fm. with the Zone Houllière, (3) the resemblance of the Feldspathic petrofacies with the Médianes Flysch and (4) a potential Briançonnais source for the andesite rock fragments.
5. Our palaeogeographic model suggests that the Voirons Flysch was fed by the reworking of the sedimentary accretionary prism (Quartzose petrofacies) including the older Prealps nappes and by intermittent inputs from the Sesia–Dent Blanche nappe and possibly from the Briançonnais (Feldspathic petrofacies). However, identifying the detritus derived from the Briançonnais basement and that originating from the Sesia–Dent Blanche nappe is not straightforward. More accurate analysis (e.g. garnet geochronology) will be necessary to emphasise the detrital inputs from the Briançonnais units.
6. Our presented palaeogeographic model for the Voirons Flysch might eventually be applied to the other flyschs of the Gurnigel nappe if future biostratigraphic studies, possibly based on planktonic foraminifers, extend the Middle Eocene to Late Eocene/Early Oligocene age

obtained for the Voirons Flysch to all deposits forming the Gurnigel nappe. Thus, further biostratigraphic investigations are urgently needed to clarify this palaeogeographic conundrum.

Acknowledgements We thank François Gischig (University of Geneva) for technical help with thin sections and Dr. Mario Sartori (University of Geneva) for fruitful conversations. We are grateful to Franz Neubauer and an anonymous reviewer for constructive comments on an earlier manuscript.

References

Ackermann A (1984) Le Flysch de la nappe du Niesen. University of Fribourg

Ackermann A (1986) Le flysch de la nappe du Niesen. Eclogae Geol Helv 79:641–684. doi:10.5169/seals-165845

Ambrosetti I (2005) Étude géologique de la région de la Valsainte (Préalpes fribourgeoises). Fribourg University

Amorosi A, Zuffa GG (2011) Sand composition changes across key boundaries of siliciclastic and hybrid depositional sequences. Sediment Geol 236:153–163. doi:10.1016/j.sedgeo.2011.01.003

Argnani A, Fontana D, Stefani C, Zuffa GG (2004) Late Cretaceous carbonate turbidites of the Northern Apennines: Shaking Adria at the onset of Alpine collision. J Geol 112:251–259. doi:10.1086/381660

Arribas J, Critelli S, Le Pera E, Tortosa A (2000) Composition of modern stream sand derived from a mixture of sedimentary and metamorphic source rocks (Henares River, Central Spain). Sediment Geol 133:27–48. doi:10.1016/S0037-0738(00)00026-9

Badoux H (1962) Géologie des Préalpes valaisannes. Matériaux pour la Cart Géologique Suisse 113:86

Badoux H (1965) Feuille et notice explicative de la Feuille Thonon–Châtel (630) de la Carte géologique de la France (1/50000ème). BRGM, Orléans

Badoux H (1996) Le substratum des Préalpes du Chablais. Bull la Société vaudoise des Sci Nat 84:113–124. doi:10.5169/seals-287992

Baker G (1962) Detrital heavy minerals in natural accumulate with special occurrence to Australian occurrences. Technical Report Monograph series n°1, Australasian Institute of Mining and Metallurgy, p 146

Baxter EF, Scherer EE (2013) Garnet geochronology: timekeeper of tectonometamorphic processes. Elements 9:433–438. doi:10.2113/gselements.9.6.433

Beltrán-Triviño A, Winkler W, Von Quadt A (2013) Tracing Alpine sediment sources through laser ablation U–Pb dating and Hf-isotopes of detrital zircons. Sedimentology 60:197–224. doi:10.1111/sed.12006

Bernoulli D, Winkler W (1990) Heavy mineral assemblages from Upper Cretaceous South- and Austroalpine flysch sequences (Northern Italy and Southern Switzerland)†¯: source terranes and palaeotectonic implications. Eclogae Geol Helv 83:287–310. doi:10.5169/seals-166588

Bertrand J, Delaloye M (1976) Datation par la méthode K-Ar de diverses ophiolites du flysch des Gets (Haute-Savoie, France). Eclogae Geol Helv 69:335–341. doi:10.5169/seals-164513

Bill M, Bussy F, Cosca M, Masson H, Hunziker JC (1997) High precision U-Pb and 40Ar/39Ar dating of an Alpine ophiolite (Gets nappe, French Alps). Eclogae Geol Helv 90:43–54. doi:10.5169/seals-168144

Bouma AH (1962) Sedimentology of some flysch deposits: a graphic approach to facies interpretation. Elsevier, Amsterdam

Broudoux B (1985) Géologie des unités de Vanoise septentrionale et méridionale de Pralognan à Tignes (Alpes de Savoie). Université des Sciences et Technologie de Lille 1

Brouwner J (1965) Agglutinated Foraminifera from some turbiditic sequences. Proc K Ned Akad van Wet Ser A 68:309–334.

Bucher S, Bousquet R (2007) Metamorphic evolution of the Briançonnais units along the ECORS-CROP profile (Western Alps): new data on metasedimentary rocks. Swiss. J Geol 100:227–242. doi:10.1007/s00015-007-1222-4

Bucher K, Grapes R (2009) The eclogite-facies Allalin gabbro of the Zermatt-Saas ophiolite, Western alps: a record of subduction zone hydration. J Petrol 50:1405–1442. doi:10.1093/petrology/egp035

Bussy F, Sartori M, Thélin P (1996) U-Pb zircon dating in the middle Penninic basement of the Western Alps (Valais, Switzerland). Schweiz Miner Petrog 76(1):81–84. doi:10.5169/seals-57689

Bütler E, Winkler W, Guillong M (2011) Laser ablation U/Pb age patterns of detrital zircons in the Schlieren Flysch (Central Switzerland): new evidence on the detrital sources. Swiss J Geosci 104:225–236. doi:10.1007/s00015-011-0065-1

Caron C (1972) La Nappe Supérieure des Préalpes: subdivisions et principaux caractères du sommet de l'édifice préalpin. Eclogae Geol Helv 65:57–73. doi:10.5169/seals-164076

Caron C (1976) La nappe du Gurnigel dans les Préalpes. Eclogae Geol Helv 69:297–308

Caron C, Homewood P, Morel R, Van Stuijvenberg J (1980) Témoins de la Nappe du Gurnigel sur les Préalpes médianes: une confirmation de son origine ultrabriançonnaise. Bull la Société fribourgeoise des Sci Nat 69:64–79. doi:10.5169/seals-308586

Caron C, Homewood P, Wildi W (1989) The original Swiss flysch: a reappraisal of the type deposits in the Swiss prealps. Earth-Science Rev 26:1–45. doi:10.1016/0012-8252(89)90002-0

Cartwright I, Barnicoat AC (2002) Petrology, geochronology, and tectonics of shear zones in the Zermatt-Saas and Combin zones of the Western Alps. J Metamorph Geol 20:263–281. doi:10.1046/j.0263-4929.2001.00366.x

Charollais J, Plancherel R, Monjuvent G, Debelmas J (1998) Notice explicative de la Carte géologique de la France (1/50000ème)—Feuille Annemasse (654). BRGM, Orléans

Cogulu E (1961) La géologie des Voirons et de la colline des Allinges. University of Geneva, Geneva

Copjaková R, Sulovský P, Paterson BA (2005) Major and trace elements in pyrope–almandine garnets as sediment provenance indicators of the Lower Carboniferous Culm sediments, Drahany Uplands, Bohemian Massif. Lithos 82:51–70. doi:10.1016/j.lithos.2004.12.006

Coppo N (1999) Géologie de la région Voirons—Vouan. University of Geneva, Geneva

Cortesogno L, Cassinis G, Dallagiovanna G, Gaggero L, Oggiano G, Ronchi A, Seno S, Vanossi M (1998) The Variscan post-collisional volcanism in Late Carboniferous–Permian sequences of Ligurian Alps, Southern Alps and Sardinia (Italy): a synthesis. Lithos 45:305–328. doi:10.1016/S0024-4937(98)00037-1

Crimes PT, Goldring R, Homewood P, van Stuijvenberg J, Winkler W (1981) Trace fossil assemblages of deep-sea fan deposits, Gurnigel and Schlieren flysch (Cretaceous-Eocene, Switzerland). Eclogae Geol Helv 74:953–995. doi:10.5169/seals-165136

Critelli S, Le Pera E, Galluzzo F, Milli S, Moscatelli M, Perrotta S, Santantonio M (2007) Interpreting siliciclastic-carbonate detrital modes in foreland basin systems: An example from Upper

Miocene arenites of the central Apennines, Italy. In: Arribas J, Critelli S, Johnsson MJ (eds) Special Paper 420: sedimentary provenance and petrogenesis: perspectives from petrography and geochemistry. Geological Society of America, pp 107–133. doi:10.1130/2006.2420(08)

Dal Piaz G, Lombardo B, Gosso G (1983) Metamorphic evolution of the Mt. Emilius Klippe, Dent Blanche nappe, Western Alps. Am J Sci 283-A:438–458

Das Gupta K, Pickering KT (2008) Petrography and temporal changes in petrofacies of deep-marine Ainsa-Jaca basin sandstone systems, Early and Middle Eocene, Spanish Pyrenees. Sedimentology 55:1083–1114. doi:10.1111/j.1365-3091.2007.00937.x

de Mortillet G (1863) Succin des Allinges. Rev Savoisienne 1:7

de Kaenel E, Salis Perch-Nielsen K von, Lindinger M (1989) The Cretaceous/Tertiary boundary in the Gurnigel Flysch (Switzerland). Eclogae Geol Helv 82:555–581. doi:10.5169/seals-166389

Decarlis A, Dallagiovanna G, Lualdi A, Maino M, Seno S (2013) Stratigraphic evolution in the Ligurian Alps between Variscan heritages and the Alpine Tethys opening: a review. Earth-Sci Rev 125:43–68. doi:10.1016/j.earscirev.2013.07.001

Dickinson WRA (1985) Interpreting Provenance Relations from Detrital Modes of Sandstones. In: Zuffa GG (ed) Provenance of Arenites. D. Reidel Publishing Compagny, Dordrecht, pp 333–361. doi:10.1007/978-94-017-2809-6_15

Dickinson WRA, Rich EI (1972) Petrologic intervals and petrofacies in the great valley sequence, Sacramento Valley, California. Geol Soc Am Bull 83:3007–3024. doi:10.1130/0016-7606(1972)83[3007:PIAPIT]2.0.CO;2

Dickinson WRA, Suczek C (1979) Plate tectonics and sandstone compositions. Am Assoc Pet Geol Bull 63:2164–2182. doi:10.1306/2F9188FB-16CE-11D7-8645000102C1865D

Dickinson WRA, Beard LS, Brakenridge GR, Erjavec JL, Ferguson RC, Inman KF, Knepp RA, Lindberg FA, Ryberg PT (1983) Provenance of North American Phanerozoic sandstones in relation to tectonic setting. Geol Soc Am Bull 94:222–235. doi:10.1130/0016-7606(1983)94<222:PONAPS>2.0.CO;2

Egger H, Homayoun M, Huber H, Rögl F, Schmitz B (2005) Early Eocene climatic, volcanic, and biotic events in the northwestern Tethyan Untersberg section, Austria. Palaeogeogr Palaeoclimatol Palaeoecol 217:243–264. doi:10.1016/j.palaeo.2004.12.006

Fabre J (1961) Contribution à l'étude de la Zone Houillère en Maurienne et en Tarentaise (Alpes de Savoie). Mem. B.R.G.M. 2:1–315

Flück W (1973) Die Flysche der praealpinen Decken im Simmental und Saanenland. Matériaux pour la Cart Géologique Suisse 146:87

Follmi KB (1990) Condensation and phosphogenesis: example of the Helvetic mid-Cretaceous (northern Tethyan margin). Geol Soc Lond Spec Publ 52:237–252. doi:10.1144/GSL.SP.1990.052.01.17

Frébourg G (2006) Les Conglomérats du Vouan: un cañon turbiditique? University of Geneva, Geneva

Füchtbauer H (1964) Sedimentpetrographische Untersuchungen in der älteren Molasse nördlich der Alpen. Eclogae Geol Helv 57:157–298. doi:10.5169/seals-163140

Gagnebin E (1944) Présence du Barrémien ultra-helvétique à St-Gingolph (Valais). Eclogae Geol Helv 37:195–197. doi:10.5169/seals-160499

Gardien V, Reusser E, Marquer D (1994) Pre-Alpine metamorphic evolution of the gneisses from the Valpelline series (Western Alps, Italy). Schweiz Miner Petrog 74:489–502. doi:10.5169/seals-56364

Garzanti E (1991) Non-carbonate intrabasinal grains in arenites: their recognition, significance, and relationship to eustatic cycles and tectonic setting. J Sediment Res 61:959–975. doi:10.1306/D4267816-2B26-11D7-8648000102C1865D

Garzanti E, Andò S (2007) Plate tectonics and heavy-mineral suites of modern sands. In: Mange M, Wright D (eds) Heavy minerals in use. Elsevier, Amsterdam, pp 741–763. doi:10.1016/S0070-4571(07)58029-5

Garzanti E, Vezzoli G (2003) A classification of metamorphic grains in sand based on their composition and grade. J Sediment Res 73:830–837. doi:10.1306/012203730830

Garzanti E, Vezzoli G, Lombardo B, Andò S, Mauri E, Monguzzi S, Russo M (2004) Collision-Orogen provenance (Western Alps): detrital signatures and unroofing trends. J Geol 112:145–164. doi:10.1086/381655

Garzanti E, Doglioni C, Vezzoli G, Andò S (2007) Orogenic belts and orogenic sediment provenance. J Geol 115:315–334. doi:10.1086/512755

Garzanti E, Resentini A, Vezzoli G, Andò S, Malusà MG, Padoan M, Paparella P (2010) Detrital fingerprints of fossil continental-subduction zones (Axial Belt Provenance, European Alps). J Geol 118:341–362. doi:10.1086/652720

Gasinski A, Slaczka A, Winkler W (1997) Tectono-sedimentary evolution of the Upper Prealps nappe (Switzerland and France): nappe formation by Late Cretaceous-Paleogene accretion. Geodin Acta 10:137–157. doi:10.1080/09853111.1997.11105299

Giorgis D, Thelin P, Stampfli G, Bussy F (1999) The Mont-Mort metapelites: Variscan metamorphism and geodynamic context (Brianconnais basement, Western Alps, Switzerland). Schweiz Miner Petrog 79:381–398. doi:10.5169/seals-60214

Gottlieb P, Wilkie G, Sutherland D, Ho-Tun E, Suthers S, Perera K, Jenkins B, Spencer S, Butcher A, Rayner J (2000) Using quantitative electron microscopy for process mineralogy applications. JOM 52:24–25. doi:10.1007/s11837-000-0126-9

Grew ES, Locock AJ, Mills SJ, Galuskina IO, Galuskin EV, Halenius U (2013) Nomenclature of the garnet supergroup. Am Miner 98:785–811. doi:10.2138/am.2013.4201

Hamilton N (2016) ggtern: an extension to "ggplot2", for the creation of ternary diagrams.

Handy MR, Schmid SM, Bousquet R, Kissling E, Bernoulli D (2010) Reconciling plate-tectonic reconstructions of Alpine Tethys with the geological–geophysical record of spreading and subduction in the Alps. Earth-Sci Rev 102:121–158. doi:10.1016/j.earscirev.2010.06.002

Henry DJ, Guidotti CV (1985) Tourmaline as a petrogenetic indicator mineral: an example from the staurolite-grade metapelites of NW Maine. Am Miner 70:1–15

Hsü JK (1960) Paleocurrent structures and paleogeography of the Ultrahelvetic flysch basins, Switzerland. Geol Soc Am Bull 71:577–610. doi:10.1130/0016-7606(1960)71[577:PSAPOT]2.0.CO;2

Hsü JK, Schlanger SO (1971) Ultrahelvetic Flysch sedimentation and deformation related to plate tectonics. Geol Soc Am Bull 82:1207. doi:10.1130/0016-7606(1971)82[1207:UFSADR]2.0.CO;2

Hubert JF (1967) Sedimentology of Prealps Flysch sequences, Switzerland. SEPM J Sediment Res 37:885–907. doi:10.1306/74D717CB-2B21-11D7-8648000102C1865D

Hunziker JC, Zingg A (1980) Lower Paleozoic Amphibolite to Granulite Facies Metamorphism im the Ivrea Zone (Southern Alps, Northern Italy. Schweiz Miner Petrog 60:181–213. doi:10.5169/seals-46667

Ingersoll RV (1978) Petrofacies and petrologic evolution of the Late Cretaceous Fore-Arc Basin, Northern and Central California. J Geol 86:335–352

Ingersoll RV (1990) Actualistic sandstone petrofacies: discriminating modern and ancient source rocks. Geology 18:733. doi:10.1130/0091-7613(1990)018<0733:ASPDMA>2.3.CO;2

Ingersoll RV, Suczek C (1979) Petrology and provenance of Neogene sand from Nicobar and Bengal Fans, DSDP Sites 211 and 218. SEPM J Sediment Res 49:1217–1228. doi:10.1306/212F78F1-2B24-11D7-8648000102C1865D

Ingersoll RV, Kretchmer AG, Valles PK (1993) The effect of sampling scale on actualistic sandstone petrofacies. Sedimentology 40:937–953. doi:10.1111/j.1365-3091.1993.tb01370.x

Jan du Chêne R (1977) Nouvelles données sur la palynostratigraphie des Flyschs des Préalpes externes (Suisse). Arch des Sci la Société Phys d'Histoire Nat Genève 30:53–63.

Jan du Chêne R, Gorin G, van Stuijvenberg J (1975) Etude géologique et stratigraphique (palynologie et nannoflore calcaire) des Grès des Voirons (Palogène de Haute-Savoie, France). Géologie Alp 51:51–78.

Jeanbourquin P, Kindler P, Dall'Agnolo S (1992) Les mélanges des Préalpes internes entre Arve et Rhône (Alpes occidentales franco-suisses). Eclogae Geol Helv 85:59–83. doi:10.5169/seals-166995

Kerrien Y, Turrel C, Monjuvent G, Charollais J, Lombard A, Balmer F, Olmari F, Papillon R, Fontannaz L, Amberger G, Ruchat C, Grebert Y, Marthaler M (1998) Feuille Annemasse (654) de la Carte géologique de la France (1/50000ème).

Kirst, F (2014) Progressive orogenic deformation and metamorphism along the Combin Fault and Dent Blanche Basal Thrust in the Swiss-Italian Western Alps. University of Bonn

Koch S, Winkler W, Von Quadt A, Ulmer P (2015) Paleocene and Early Eocene volcanic ash layers in the Schlieren Flysch, Switzerland: U–Pb dating and Hf-isotopes of zircons, pumice geochemistry and origin. Lithos 236–237:324–337. doi:10.1016/j.lithos.2015.07.008

Krippner A, Meinhold G, Morton AC, von Eynatten H (2014) Evaluation of garnet discrimination diagrams using geochemical data of garnets derived from various host rocks. Sediment Geol 306:36–52. doi:10.1016/j.sedgeo.2014.03.004

Kuenen PH, Carozzi AV (1953) Turbidity currents and sliding in geosynclinal basins of the Alps. J Geol 61:363–373. doi:10.1086/626101

Kuhn JA (1972) Stratigraphisch-mikropaläontologische Untersuchungen in der Äusseren Einsiedler Schuppenzone und im Wägitaler Flysch E und W des Sihlsees (Kt. Schwyz). Eclogae Geol Helv 65:485–533. doi:10.5169/seals-164104

Lihou JC, Mange-Rajetzky MA (1996) Provenance of the Sardona Flysch, eastern Swiss Alps: example of high-resolution heavy mineral analysis applied to an ultrastable assemblage. Sediment Geol 105:141–157. doi:10.1016/0037-0738(95)00147-6

Lombard A (1940) Géologie des Voirons. Mémoire la Société helvétique des Sci Nat 74:118p.

Mack GH (1984) Exceptions to the relationship between plate tectonics and sandstone composition. J Sediment Res 54:212–220. doi:10.1306/212F83E6-2B24-11D7-8648000102C1865D

Mange MA, Maurer HFW (1992) Heavy minerals in colour. Chapman & Hall, London

Mange MA, Morton AC (2007) Geochemistry of heavy minerals. In: Mange MA, Wright DT (eds) Heavy minerals in use. Elsiever, Amsterdam, pp 345–391. doi:10.1016/S0070-4571(07)58013-1

Manzotti P, Ballèvre M, Zucali M, Robyr M, Engi M (2014) The tectonometamorphic evolution of the Sesia–Dent Blanche nappes (internal Western Alps): review and synthesis. Swiss J Geosci 107:309–336. doi:10.1007/s00015-014-0172-x

Manzotti P, Ballèvre M, Poujol M (2016) Detrital zircon geochronology in the Dora-Maira and Zone Houillère: a record of sediment travel paths in the Carboniferous. Terra Nova 28:279–288. doi:10.1111/ter.12219

Morad S, Bergan M, Knarud R, Nyusten JP (1990) Albitization of Detrital Plagioclase in Triassic Reservoir Sandstones from the Snorre Field, Norwegian North Sea. J Sediment Res 60:411–425. doi:10.1306/212F91AB-2B24-11D7-8648000102C1865D

Morad S, Ketzer JM, De Ros LF (2000) Spatial and temporal distribution of diagenetic alterations in siliciclastic rocks: implications for mass transfer in sedimentary basins. Sedimentology 47:95–120. doi:10.1046/j.1365-3091.2000.00007.x

Morel R (1980) Géologie du massif du Niremont (Préalpes romandes) et de ses abords. Bull la Société fribourgeoise des Sci Nat 69:99–207. doi:10.5169/seals-308588

Morton AC, Hallsworth CR (1994) Identifying provenance-specific features of detrital heavy mineral assemblages in sandstones. Sediment Geol 90:241–256. doi:10.1016/0037-0738(94)90041-8

Morton AC, Hallsworth CR (1999) Processes controlling the composition of heavy mineral assemblages in sandstones. Sediment Geol 124:3–29. doi:10.1016/S0037-0738(98)00118-3

Mosar J (1991) Géologie structurale dans les Préalpes Médianes (Suisse). Eclogae Geol Helv 84:689–725

Mosar J, Stampfli G, François G (1996) Western Préalpes Médianes Romandes: timing and structure: a review. Eclogae Geol Helv 89:389–425

Norman MB (1974) Improved techniques for selective staining of feldspar and other minerals using amaranth. J Res US Geol Surv 2:73–79

Notholt AJG, Sheldon RP, Davidson DF (1989) Phosphate deposits of the world. Volume 2. Phosphate rock resources. Cambridge University Press, Cambridge

Oberhänsli R (1980) PT Bestimmungen anhand von Mineralanalysen in Eklogiten und Glaukophaniten der Ophiolite von Zermatt. Schweiz Miner Petrog 60:215–235. doi:10.5169/seals-46668

Odin G, Matter A (1981) De glauconiarum origine. Sedimentology 28(5):611–641. doi:10.1111/j.1365-3091.1981.tb01925.x

Ospina-Ostios LM (2017) Biostratigraphy and Structure of the Voirons Flysch (Gurnigel Nappe, Haute-Savoie, France). University of Geneva (unpublished)

Ospina-Ostios LM, Ragusa J, Wernli R, Kindler P (2013) Planktonic foraminifer biostratigraphy as a tool in constraining the timing of flysch deposition: Gurnigel flysch, Voirons massif (Haute-Savoie, France). Sedimentology 60:225–238. doi:10.1111/sed.12013

Picard MD, McBride EF (2007) Comparison of river and beach sand composition with source rocks, Dolomite Alps drainage basins, northeastern Italy. Geol Soc Am Sp Papers 420:1–12. doi:10.1130/2007.2420(01)

Pilloud J (1936) Contribution à l'étude stratigraphique des Voirons. Préalpes externes, Haute-Savoie. Arch des Sci la Société Phys d'Histoire Nat Genève 18:219–249.

R Core Team (2015) R: a language and environment for statistical computing

Ragusa J (2009) Études des populations de minéraux lourds dans les Flyschs des Voirons et les Grès de Samoëns. University of Geneva (unpublished)

Ragusa J (2015) Pétrographie, stratigraphie et provenance du Flysch des Voirons (Nappe du Gurnigel, Haute-Savoie, France). University of Geneva (unpublished)

Renevier E (1893) Géologie des Préalpes de la Savoie. Eclogae Geol Helv 4(1):53–73. doi:10.5169/seals-154920

Rigassi D (1958) Foraminifères des "Grès des Voirons." Arch des Sci la Société Phys d'Histoire Nat Genève 11:398–400.

Sarasin C (1894) De l'origine des blocs exotiques du Flysch. Arch des Sci la Société Phys d'Histoire Nat Genève 32:67–101.

Sartori M, Gouffon Y, Marthaler M (2006) Harmonisation et définition des unités lithostratigraphiques briançonnaises dans les nappes penniques du Valais. Eclogae Geol Helv 99:363–407. doi:10.1007/s00015-006-1200-2

Schaltegger U, Gebauer D (1999) Pre-Alpine geochronology of the Central, Western and Southern Alps. Schweiz Miner Petrog 79:79–87. doi:10.5169/seals-60199

Schertl HP, Schreyer W, Chopin, C (1991) The pyrope-coesite rocks and their country rocks at Parigi, Dora Maira Massif, Western Alps: detailed petrography, mineral chemistry and PT-path. Contrib Miner Petrol 108:1–21. doi:10.1007/BF00307322

Schmid SM, Pfiffner OA, Froitzheim N, Schönborn G, Kissling E (1996) Geophysical-geological transect and tectonic evolution of the Swiss-Italian Alps. Tectonics 15:1036–1064. doi:10.1029/96TC00433

Schmid SM, Fügenschuh B, Kissling E, Schuster R (2004) Tectonic map and overall architecture of the Alpine orogen. Eclogae Geol Helv 97:93–117. doi:10.1007/s00015-004-1113-x

Stampfli GM, Borel GD (2002) A plate tectonic model for the Paleozoic and Mesozoic constrained by dynamic plate boundaries and restored synthetic oceanic isochrons. Earth Planet Sci Lett 196:17–33. doi:10.1016/S0012-821X(01)00588-X

Stampfli G, Mosar J, Marquer D, Marchant R, Baudin T, Borel G (1998) Subduction and obduction processes in the Swiss Alps. Tectonophysics 296:159–204. doi:10.1016/S0040-1951(98)00142-5

Stampfli GM, Borel GD, Marchant R, Mosar J (2002) Western Alps geological constraints on western Tethyan reconstructions. In: Rosenbaum G, Lister GS (eds) Reconstruction of the evolution of the Alpine-Himalayan Orogen. Journal of the Virtual Explorer, pp 75–104. doi:10.3809/jvirtex.2002.00057

Stefani C, Zattin M, Grandesso P (2007) Petrography of Paleogene turbiditic sedimentation in northeastern Italy. In: Arribas J, Critelli S, Johnsson MJ (eds) Sedimentary provenance and petrogenesis: perspectives from petrography and geochemistry. Geological Society of America, pp 37–55. doi:10.1130/2007.2420(04)

Stutenbecker L, Berger A, Schlunegger, F (2016) Detrital garnet fingerprint of the Central Swiss Alps. Swiss Geological Meeting.

SwissTopo (2008) Carte géologique et tectonique de la Suisse au 1:500′000.

Tercier J (1928) Géologie de la Berra. Matériaux pour la Cart Géologique Suisse 60

Thélin P, Sartori M, Lengeler R, Schaerer JP (1990) Eclogites of Paleozoic or early Alpine age in the basement of the Penninic Siviez-Mischabel nappe, Wallis, Switzerland. Lithos 25:71–88. doi:10.1016/0024-4937(90)90007-N

Trautwein B, Dunkl I, Frisch W (2001) Accretionary history of the Rhenodanubian flysch zone in the Eastern Alps—evidence from apatite fission-track geochronology. Int J Earth Sci 90:703–713. doi:10.1007/s005310000184

Trümpy R (1960) Paleotectonic evolution of the central and western Alps. Geol Soc Am Bull 71:843–908. doi:10.1130/0016-7606(1960)71[843:PEOTCA]2.0.CO;2

Trümpy R (2006) Geologie der Iberger Klippen und ihrer Flysch-Unterlage. Eclogae Geol Helv 99:79–121. doi:10.1007/s00015-006-1180-2

Ujetz B (1996) Micropaleontology of Paleogene deep water sediments, Haute-Savoie, France. University of Geneva, Geneva

Van Stuijvenberg J (1979) Geology of the Gurnigel area (Prealps, Switzerland). Matériaux pour la Carte Géologique Suisse 151

Van Stuijvenberg J (1980) Stratigraphie et structure de la Nappe du Gurnigel aux Voirons, Haute-Savoie. Bull la Société fribourgeoise des Sci Nat 69(1):80–96. doi:10.5169/seals-308587

Van Stuijvenberg J, Jan du Chêne R (1980) Nouvelles observations stratigraphiques dans le massif des Voirons. Bull du BRGM 1:3–9.

Van Stuijvenberg J, Morel R, Jan du Chêne R (1976) Contribution à l'étude des flyschs de la région de Fayaux (Préalpes externes vaudoises). Eclogae Geol Helv 69:309–326. doi:10.5169/seals-164511

Van der Plas L (1962) Preliminary note on the granulometric analysis of sedimentary rocks. Sedimentology 1:145–157. doi:10.1111/j.1365-3091.1962.tb00031.x

Velbel MA (1985) Mineralogically mature sandstones in accretionary prisms. J Sediment Petrol 55:685–690. doi:10.1306/212F87BA-2B24-11D7-8648000102C1865D

Venturelli G, Thorpe RS, Dal Piaz GV, Del Moro A, Potts PJ (1984) Petrogenesis of calc-alkaline, shoshonitic and associated ultrapotassic Oligocene volcanic rocks from the Northwestern Alps, Italy. Contrib Mineral Petrol 86:209–220. doi:10.1007/BF00373666

Vial R, Conrad MA, Charollais J (1989) Notice explicative de la Feuille Douvaine (629) de la Carte géologique de la France (1/50000ème). BRGM, Orléans

von Eynatten H, Dunkl I (2012) Assessing the sediment factory: the role of single grain analysis. Earth-Science Rev 115:97–120. doi:10.1016/j.earscirev.2012.08.001

von Eynatten H, Gaupp R (1999) Provenance of Cretaceous synorogenic sandstones in the Eastern Alps—constraints from framework petrography, heavy mineral analysis and mineral chemistry. Sediment Geol 124:81–111. doi:10.1016/S0037-0738(98)00122-5

Weber S, Bucher K (2015) An eclogite-bearing continental tectonic slice in the Zermatt–Saas high-pressure ophiolites at Trockener Steg (Zermatt, Swiss Western Alps). Lithos 232:336–359. doi:10.1016/j.lithos.2015.07.010

Weidmann M (1967) Petite contribution à la connaissance du flysch. Bull des Lab Géologie l'Université Lausanne 166:1–6

Weidmann M (1985) Géologie des Pléiades. Bull la Société vaudoise des Sci Nat 77:195–204. doi:10.5169/seals-278511

Weidmann M, Morel R, Van Stuijvenberg J (1976) La nappe du Gurnigel entre la Baye de Clarens et la Veveyse de Châtel. Bull la Société fribourgeoise des Sci Nat 65:182–196. doi:10.5169/seals-308540

Weltje GJ (2002) Quantitative analysis of detrital modes: statistically rigorous confidence regions in ternary diagrams and their use in sedimentary petrology. Earth-Science Rev 57:211–253. doi:10.1016/S0012-8252(01)00076-9

Whitney DL, Evans BW (2010) Abbreviations for names of rock-forming minerals. Am Miner 95:185–187. doi:10.2138/am.2010.3371

Wildi W (1985) Heavy mineral distribution and dispersal pattern in penninic and ligurian flysch basins (Alps, northern Apennines). G di Geol 47:77–99.

Win KS, Takeuchi M, Iwakiri S, Tokiwa T (2007) Provenance of detrital garnets from the Yukawa Formation, Yanase district, Shimanto belt, Kii Peninsula, Southwest Japan. J Geol Soc Japan 113:133–145. doi:10.5575/geosoc.113.133

Winkler W (1983) Stratigraphie, Sedimentologie und Sediment-petrographie des Schlieren-Flysches (Zentralschweiz). Matériaux pour la Cart Géologique Suisse 158:115

Winkler W (1984) Paleocurrents and petrography of the Gurnigel-Schlieren flysch: a basin analysis. Sediment Geol 40:169–189. doi:10.1016/0037-0738(84)90045-9

Winkler W (1993) Control factors on turbidite sedimentation in a deep-sea trench setting—the example of the Schlieren Flysch (Upper Maastrichtian-Lower Eocene, Central Switzerland). Geodin Acta 6:81–102. doi:10.1080/09853111.1993.11105240

Winkler W, Galetti G, Maggetti M (1985a) Bentonite im Gurnigel-, Schlieren- und Wägital Flysch: Mineralogie, Chemismus, Herkunft. Eclogae Geol Helv 78:545–564. doi:10.5169/seals-165670

Winkler W, Wildi W, Van Stuijvenberg J, Caron C (1985b) Wägital-Flysch et autres flyschs pennique en Suisse Centrale.

Stratigraphie, sédimentologie et comparaisons. Eclogae Geol Helv 78:1–22. doi:10.5169/seals-165641

Winkler W, Hurford AJ, von Salis Perch-Nielsen K, Odin GS (1990) Fission track and nannofossil ages from a Palaeocene bentonite in the Schlieren Flysch (Central Alps, Swistzerland). Schweiz Miner Petrog 70:389–396. doi:10.5169/seals-53629

Wissing SB, Pfiffner AO (2002) Structure of the eastern Klippen nappe (BE, FR)†¯: implications for its Alpine tectonic evolution. Eclogae Geol Helv 95:381–398. doi:10.5169/seals-168966

Young SW (1976) Petrographic texture of detrial polycrystalline quartz as an aid to interpreting crystalline source rocks. J Sediment Petrol 46:595–603. doi:10.1306/212F6FFA-2B24-11D7-8648000102C1865D

Zuffa GG (1980) Hybrid arenites: their composition and classification. J Sediment Petrol 50:21–29. doi:10.1306/212F7950-2B24-11D7-8648000102C1865D